# UC Irvine
## UC Irvine Electronic Theses and Dissertations

**Title**

Fabrication and Testing of a Neuronal Coculture Device and Hydrophoretic Cell Sorting Device via Multi-Layer Dry Resist Laminate Photolithography

**Permalink**

https://escholarship.org/uc/item/7nt0c5nh

**Author**

KOUCHERIAN, NAREK EDWARD

**Publication Date**

2022

Peer reviewed|Thesis/dissertation

UNIVERSITY OF CALIFORNIA

IRVINE

Fabrication and Testing of a Neuronal Coculture Device and Hydrophoretic Cell Sorting Device

via Multi-Layer Dry Resist Laminate Photolithography

THESIS

Submitted in partial satisfaction of the requirements

for the degree of

MASTER OF SCIENCE

in Biomedical Engineering

by

Narek Koucherian

Thesis Committee:

Associate Professor Elliot Hui, Chair

Chancellor's Professor Abraham Lee

Assistant Professor Christopher James Halbrook

2022

## DEDICATION

To my parents, sister, girlfriend, family, and friends,

for their support and patience.

**TABLE OF CONTENTS**

# LIST OF FIGURES

# LIST OF TABLES

# ACKNOWLEDGEMENTS

# ABSTRACT OF THE THESIS

Fabrication and Testing of a Neuronal Coculture Device and Hydrophoretic Cell Sorting Device

via Multi-Layer Dry Resist Laminate Photolithography

By

Narek Koucherian

Master of Science in Biomedical Engineering

University of California, Irvine, 2022

Associate Professor Elliot Hui, Chair

PDMS (polydimethylsiloxane) devices are important for several complex microfluidic applications. The molds used to create these devices are commonly made with SU-8 liquid photoresists, however, dry film photoresists are increasingly gaining ground in similar applications. In this work, we present a multi-layer dry resist lamination photolithography fabrication procedure for the development of microfluidic device molds. Here, we report a method to achieve alignment within ~50-µm of error for two-layer devices using ADEX or SUEX photoresists ranging from 10um to 300-µm in thickness. This method is advantageous for not requiring a clean room setting and using standardized height dry film photoresists for easy mold replicability.

Multilayer alignment typically requires the first layer to be developed before adding the second, so that first-layer features are visible to allow alignment of the second layer. This works fine with liquid resists such as SU-8, which can flow over the topography of the fully developed first layer. However, dry film resists must be laminated onto a flat surface. Here, we demonstrate

that mask patterns can be revealed by an appropriately designed post-exposure bake, without using developer, leaving an intact first layer of resist that allows lamination of a second layer. 50-μm alignment accuracy was achieved between first and second layer patterns without the use of a mask aligner. This fabrication method was used to create two microfluidic devices with multi-layer architecture, a neuronal coculture chemotaxis device and a hydrophoretic cell sorting device.

Cancer organoids are three-dimensional tissues that can be grown from patient biopsy material or tumor fragments that are dissociated and embedded in Matrigel or similar basement membrane extracts. Organoids can be used for rapid drug screening of patient derived cancer cells to develop cancer therapy and treatment options more efficiently for patients. Conventional organoid preparations require substantial amounts of patient-derived tissue per experimental condition, forcing months of culture expansion that can be detrimental to patients with rapidly progressing tumors. The use of a droplet generator to culture organoids into smaller Matrigel beads would increase the drug screening rate, reduce costs, and increase the accuracy of screenings. In this work, a hydrophoretic cell sorting device was developed to group cancer cells and cell clusters ranging up to 250um in diameter into similar sized categories. The grouping of cells in this manner would aid in the consistent generation of uniform cancer organoids. Here, we discuss the development and testing of the hydrophoretic cell sorting device and test a droplet generation device to encapsulate cancer cells in Matrigel which are later grown into organoids.

Chapter 1: Introduction

    1.1 <u>Multi-Layer Microfluidic Device Fabrication</u>

    Soft lithography is the most popular method of microfluidic device fabrication. It involves the preparation of a mold/masters upon which PDMS can be repeatedly cast and hardened to obtain reproducible copies of a microfluidic device.  Many microfluidic devices include complex, multi-layer architecture which allows for unique functionality. Two such examples of these devices are multi chamber coculture devices [1,2,3] and hydrophoretic size-based cell sorting devices [4,5]. Multi-layer lithography differs from conventional lithography by incorporating unique photomasks for each layer. These masks enable different designs to be patterned onto each layer, allowing for complex architecture. Each layer is patterned with alignment markers, to help align subsequent layers through the semitransparent photoresists.

    The most common method of mold production involves the use of SU-8 liquid negative photoresists. For this method, each layer of the SU-8 mold must individually be spin coated, soft baked, exposed, developed, and hard baked prior to the application of new SU-8 for the subsequent layer designs [6]. Once an initial layer is developed, its structures become visible. Newly added SU-8 liquid resist can then flow over the topography of the first layer and create the second layer. Second layer photomask features can then be aligned to the outstanding developed first layer features visible through the second layer semi-transparent resist.

    As an alternative to SU-8 resists, dry film negative photoresists such as ADEX and SUEX, carry certain advantages for use in multi-layer lithography [7,8]. Dry film photoresists are produced with standardized layer thicknesses for easy fabrication reproducibility. Instead of spin coating, dry film photoresists are laminated onto silicon wafers by using hot rollers. Unlike

the SU-8 method, dry resist layers cannot be individually developed since the lamination of a second layer would flatten and damage the structures of the first layer. Due to these types of unique challenges associated with dry resist films, multi-layer dry resist photolithography has never been accomplished.

In this work, we present a novel method of multi-layer photolithography using dry film photoresist lamination. In our procedure, an initial dry resist layer can be partially baked after exposure to reveal device patterns and critical alignment features while leaving an intact first layer that allows the lamination of a second layer. Subsequent layers of dry film photoresists can be directly laminated atop the previous layer after the post exposure bake step, eliminating the need for multiple rounds of development and hard baking. Afterwards, a new photomask can be used to introduce different patterning for the second layer. Since dry film photoresists range from transparent to semitransparent (within the 10um-300um thickness range), alignment markers can be patterned onto the first layer of photoresist to help align the second layer mask and pattern. Our procedure is low cost, easily accessible, and allows for hand alignment of layers with the aid of a microscope. This procedure is useful for the development of devices where alignment accuracy error between layers can be within ~50um. In the proposed hand alignment method, multiple sizes of markers are used with features ranging from 10um to 1mm. Larger marker features are used to align layers by eye, while smaller features are used to fine tune and verify the alignment accuracy with the use of a microscope.

### 1.2 Neuronal Coculture Chemotaxis Device

Of the two device designs employed to test the multi-layer fabrication method, the first design was that of a Neuronal Coculture device. The device is intended to study the migration of microglia from an external annular chamber towards neurons and chemoattractants located inside

a central chamber. Previous work has shown that interactions between microglia and neuronal cells can lead to phosphorylated tau and amyloid-beta plaque accumulation. Development of this plaque in-vitro serves as an analogue for researchers to investigate the underlying mechanisms of Alzheimer's disease [9]. Patients with Alzheimer's experience similar plaque accumulation in their hippocampus region, which leads to memory loss and many other complications associated with the disease.

In this design, the microglia must migrate across chambers using narrow 10um x 50um x 100um microchannels. The 10um height restriction of the design's first layer requires the use of thin ADEX dry film photoresists for this device. A great degree of accuracy was required in the multi-layer alignment of this device to ensure all microchannels fit evenly between the annular and central chambers while maintaining near equivalent lengths of 100um.

### 1.3 Hydrophoretic Cell Sorting Device

After testing the multi-layer fabrication method on the neuronal coculture device, a hydrophoretic cell sorting device was fabricated. The aim of this device was to employ a natural sorting method known as Hydrophoresis to sort and group patient derived cancer cell and cell clusters into similar size categories ranging up to 250um in diameter. While similar devices had been produced in works by Je-Kyun Park and Sungyung Choi [10], the devices had never been scaled up to accommodate particles with an upper size limit of 250um in diameter. The key design principle in Hydrophoresis is the use of slanted trench like grooves running along a central channel. The dimensions and angles of these grooves, combined with the height and width of the main channel allow for the establishment of liquid flow patterns, forcing larger particles to be sorted laterally downwards while smaller particles such as single cells are sorter laterally upwards.

The design of the hydrophoretic filter emphasizes the need for accuracy in the multi-layer alignment process. For the design used in this study, 175 700um wide grooves span the length of the device's 800um wide main channel, resulting in a maximum allowable alignment error of 50um in the flat planar y-axis of the device.

1.4 <u>Droplet Generation Device</u>

The primary reason for developing a hydrophoretic filter was to sort cancer cells and cell clusters which would be used to create patient derived cancer organoids. To accomplish this, uniform sized groups of cells would be combined with a droplet generation device produced by Dr. David Eddington's lab at the University of Illinois, Chicago to grow organoids from cancer cells encapsulated in Matrigel, a basement membrane extracellular matrix [11]. Cancer organoids can be used to rapidly test various drug therapy treatments on patient derived cancer cells. [12,13]. It is crucial to reduce the duration of the drug screening process as much as possible to prevent a patient's cancer from progressing into late stages.

In this study, the droplet generation device from Dr. Eddington's lab was tested. Initial trials were conducted with the omission of cancer cells, resulting in pure Matrigel beads being produced. Later trials were able to successfully encapsulate cancer cells inside Matrigel droplets, which later grew into cancer organoids.

Chapter 2: Neuronal Coculture Device Fabrication and Testing

## 2.1 Background and Previous Work

Alzheimer's disease is the world's leading cause of age-related neurodegeneration [1]. Patients of Alzheimer's disease undergo neuroinflammation and have increased levels of amyloid-beta plaques, phosphorylated tau expression, and microglial marker expression which leads to neuronal death and dysfunction [14,15]. To better understand the mechanisms of Alzheimer's disease, researchers have attempted to recreate the cellular interactions that cause the expression of these factors in vitro using microfluidic neuronal chemotaxis devices. Previous works have demonstrated the creation of these coculture devices using SU-8 liquid photoresists with sequential patterning techniques [2].

## 2.2 Design Considerations

In this work, we recreated the neuronal coculture chemotaxis device using multi-layer dry resist photolithography with thin ADEX photoresists ranging from 10um to 50um in layer height (thickness).
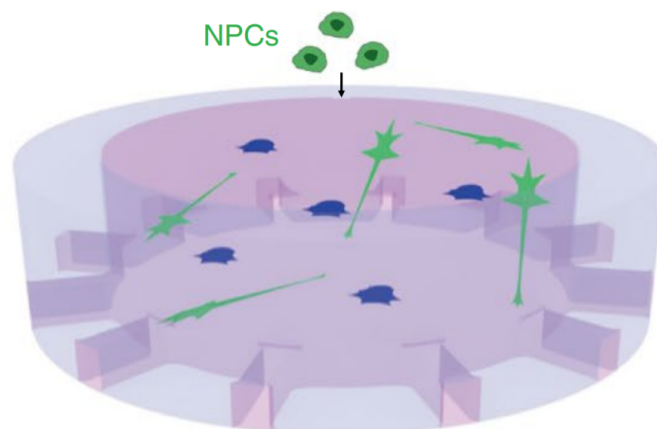


**Figure 2.1** Schematic of 3D neuronal chemotaxis device [1].

The design depicts a central chamber where neuronal cells, precursors (NPCs), and chemo-attractants will be injected. The annular or outer chamber (not depicted) is separated by several microchannels between the two chambers. Microglia are injected into the annular chamber and gradually migrate inward through the microchannels to the central chamber due to a chemical gradient being present. In this work, the microchannel dimensions were Height:10um x Width:50um x Lenght:100um.
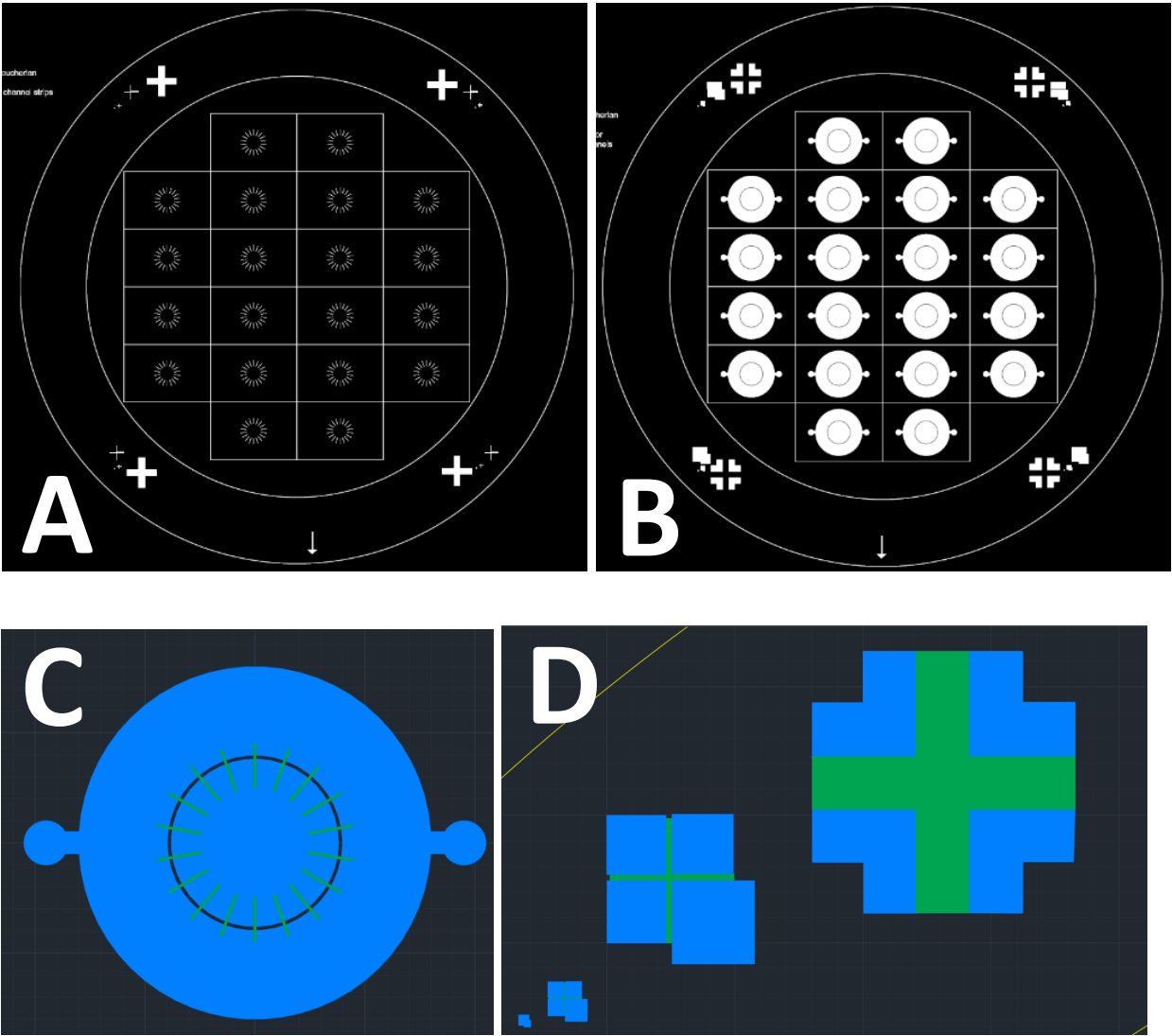
**Figure 2.2** Photomasks used for creation of neuronal coculture devices. (A) First layer photomask used to make microchannel structures. (B) Second layer photomask used to form central and annular chambers with inlets and outlets. (C) AutoCAD drawing of overlayed first- and second-layer features of a unit neuronal coculture device. First layer microchannels are shown in green, second layer annular and central chambers are shown in blue. (D) AutoCAD drawing of overlayed first- and second-layer alignment markers from top left corner of photomasks. First layer cross markers are shown in green while second layer crosshair markers are shown in blue.

Two dark-field photomasks were used to construct the complex architecture required for the neuronal coculture device. The photomasks were designed using AutoCAD and printed from CADart services with a minimum feature accuracy of 8um. The design of these masks permitted the creation of 20 units of the device. The first mask **Figure 2.2a** includes the microchannel designs used for the 10um tall layer. Despite the final microchannel lengths being 100um, the first layer microchannel features were set at 1000um to allow for misalignment error. The second mask **Figure 2.2b** includes the central and annular chamber designs used for the 100um tall layer. Inner chamber diameter was 3.8mm, while the outer chamber diameter was 8mm. Chamber diameters were chosen in accordance with the device height to create a central chamber with a minimum volume of 1uL, and an annular chamber with a minimum volume of 4uLs. The negative 100um ringed area between the two chambers was meant to be aligned directly atop the microchannels of the first layer to capture their design. The remaining 900um lengths of the channels would be exposed into the areas of the central and annular chambers. It is crucial for the alignment accuracy error between layers to be minimal to ensure evenly spaced and angled microchannels are fabricated for each unit device.

Two inlets are included on the sides of the annular chamber. Alignment markers used for this set of masks include the crosses on the first layer and crosshairs on the second layer. Each "corner" of the device had a set of 4 alignment markers. Larger markers were used for naked-eye hand alignment, while smaller markers were used for precision alignment under the microscope, measuring down to 10um feature length.

2.3 <u>Device Fabrication</u>

Device assembly began with the lamination of the first layer dry film photoresist. A clean 100mm diameter silicon wafer was obtained. The first protective layer of photoresist (glossy side for SUEX, "X" marked side for ADEX) was separated and peeled off using a sharp blade edge. The lamination assembly begins with the following items stacked atop each other in order:

1) A steel carrier sheet base

2) The 100mm diameter silicon wafer

3) A thin plastic spacer sheet covering all but the top inch of the wafer's surface

4) The 96mm diameter, 10um thick ADEX photoresist with the peeled-off side face down, contacting the wafer at the 1-inch opening

5) A second protective plastic sheet placed atop the whole assembly to prevent the photoresist from adhering to or damaging the laminator.

The layered assembly was run through the laminator (SKY, 335R6 Photo Pouch Laminator) at a speed of 3 at 70⁰C. Care was taken to hold back the spacer sheet as the assembly was fed through the laminator, allowing the photoresist and wafer to adhere to each other. The wafer was allowed to cool to room temperature before advancing to the exposure step.

Next, the second protective layer of the photoresist (hazy side for SUEX, numbered side for ADEX) was separated and peeled off using a sharp blade edge. The first layer photomask was assembled atop the first layer photoresist. A 4x4 glass slide was placed atop the assembly to flatten the photomask. Exposure was performed in a dark room. The photoresist was allowed to rest in a dark area for least 2 hours after exposure to permit adequate time for crosslinking of exposed photoresist features. The following table lists the UV light exposure durations for each layer of the neuronal coculture device.

| Device Layers | Photoresist Height | Exposure Duration |
|---------------|--------------------|-------------------|
| Layer 1 | 10um (ADEX) | 1 minute |
| Layer 2 | 2x50um (ADEX) | 4 minutes |

**Table 2.1** UV exposure durations for optimized feature development of the neuronal coculture device.

After initial exposure, a post exposure bake (PEB) was performed on the first layer of photoresist to reveal and highlight key exposed features in the microchannel and alignment marker patterns. The visibility of first layer alignment markers is necessary to enable the accurate alignment of first layer features to the second layer photomask patterns. The following table lists the PEB procedure for each layer of the neuronal coculture device.

| Device Layer | Photoresist Height | PEB Procedure |
|---|---|---|
| Layer 1 | 10um (ADEX) | 1) Pre-heat oven to 95⁰C<br>2) Bake at 95⁰C for 5 mins<br>3) Turn off oven with wafer inside and naturally cool wafer to room temperature |
| Layer 2 | 2x 50um (ADEX) | 1) Pre-heat oven to 95⁰C<br>2) Bake at 95⁰C for 12 mins<br>3) Turn off oven with wafer inside and naturally cool wafer to room temperature |

**Table 2.2** PEB procedures for each layer of the neuronal coculture device

PEB times are directly correlated to layer thickness. ADEX photoresist layers range from thicknesses of 10um to 75um and require shorter PEB duration. SUEX photoresists are generally thicker than 100um and more sensitive to rapid fluctuations in temperature, thus requiring longer temperature ramp up and cool down periods. Rapid changes in temperature may cause deformation of exposed features on the surface of the photoresist. While feature deformation was not an issue for the fabrication of an ADEX based device, we will later see how it could adversely affect SUEX based device fabrication.

Following the initial PEB, a second set of photoresists were laminated onto the wafer. Due to the volume requirements of the annular and central chambers, a minimum height of 90um was required for the features of the second layer, as this would combine with the unexposed 10um tall sections of the first layer to create a total height of 100um for the two chambers. DJMicrolaminates, the supplier of ADEX and SUEX photoresist products, only provides ADEX dry resist sheets in set sizes of 5, 10, 20, 25, 30, 40, 50 and 75um thickness [16]. Thus, two 50um sheets were chosen to create a combined height of 100um for the second layer (110um for the total device height). ADEX and SUEX circular photoresists can also vary in total resist diameter and are available in set diameter lengths of 48, 73, 96, 146, 196, and 296mm. Although the

circular photoresist used for the initial 10um tall layer had a diameter of 96mm, the second set of 50um tall photoresists had diameters of 73um to permit the visibility of first layer alignment markers located on the edge of the outer 23mm ring of the first layer shown in **Figure 2.2**.

The second layer lamination procedure was conducted similarly to that of the first layer. After peeling of the "X" marked protective layer of the first 50um photoresist, the resist was placed atop the wafer with the first layer photoresist already laminated on following the same lamination assembly. After laminating the first 50um thick layer, its second protective sheet was peeled off, and a second 50um thick photoresist was laminated atop the initial 50um layer in the same way. Care was taken to properly align the two 50um layers to prevent the fracturing of misaligned and overhanging sections of the photoresist sheet. In this scenario, misalignment and overhang refers to when the top layer of photoresist has a section that is unsupported and suspended in the air by not having the preceding layer's photoresist occupy the area directly underneath it. These overhanging edge areas will get crushed and fractured due to the pressure applied by the laminator rollers.

After removing the topmost protective sheets on the second layer of laminated photoresists, the alignment markers found on the first layer should become partially visible through the second layer of unexposed, semi-transparent photoresist. Thinner photoresists such as ADEX allow for easier visibility of the first layer alignment markers. Thicker photoresists such as SUEX will still allow for the visibility of the first layer alignment markers through the second layer of photoresist, but not to the extent of clarity provided by thinner ADEX material.

With the aid of the first layer alignment markers, the second layer photomask was positioned atop the assembled wafer and aligned. The larger markers were manually hand aligned by eye, while smaller markers were aligned and verified using a microscope. Binder clips

were used to hold the assembly together and maintain photomask alignment. A 4x4 glass slide

filter was placed atop the assembly to keep the photomask flat. Exposure was performed in a

dark room. The photoresist was allowed to rest in a dark area for at least 2 hours after exposure

to permit adequate time for crosslinking of exposed photoresist features. Table 2.1 shows the

durations used for the second rounds of UV exposure.
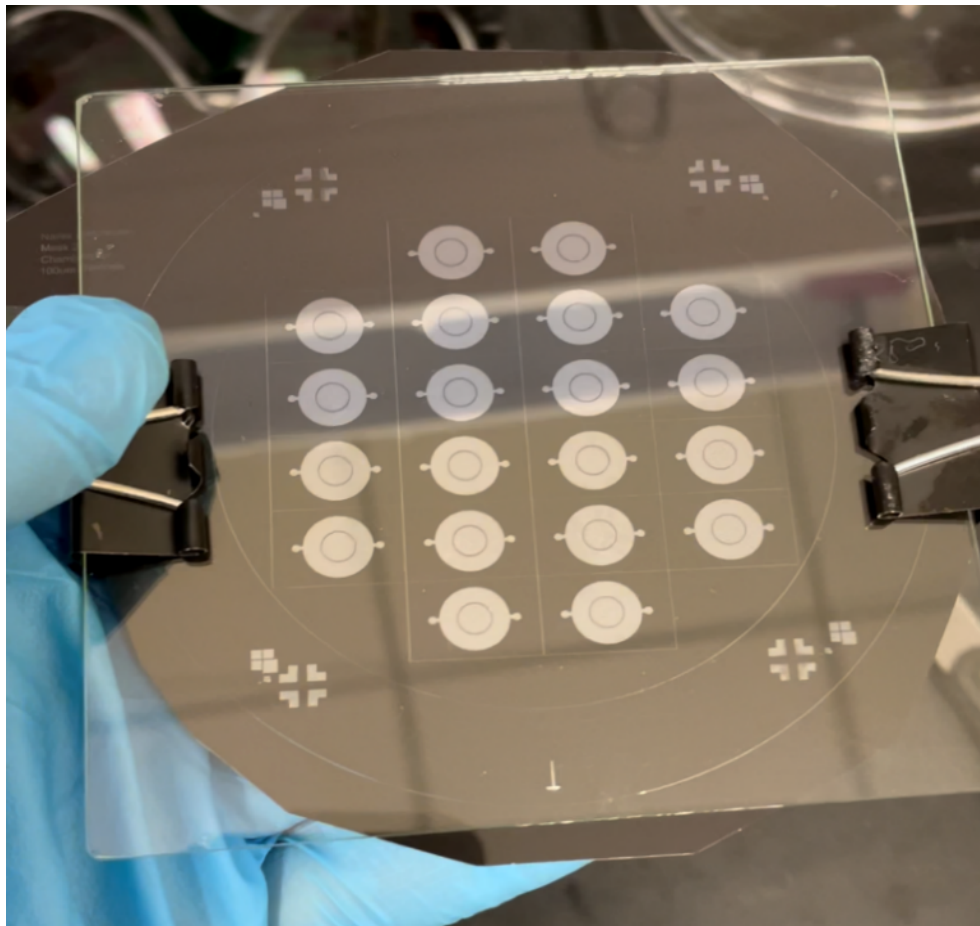


**Figure 2.3** Multi-Layer alignment assembly used for second layer exposure of the

neuronal coculture device
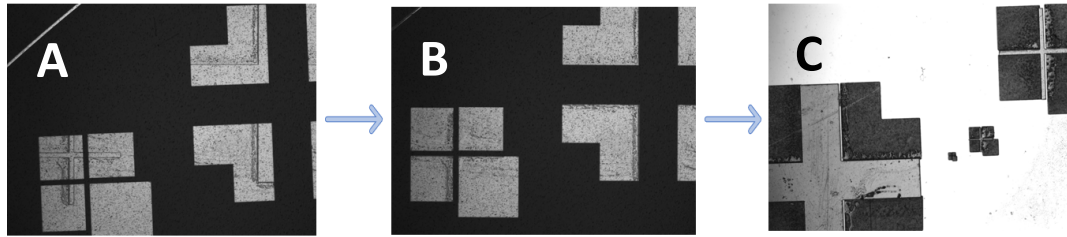
**Figure 2.4** Alignment procedure of photomasks shown under microscope view. (A) Greater than 500um in misalignment error was shown. (B) Second layer photomask and first layer alignment markers are more accurately aligned to achieve less than 50um in alignment error. (C) Cross and crosshair alignment marker pairs shown on the device mold after the second PEB. Four markers were used in each corner of the device with spoke widths ranging from 1mm down to 10um. First layer crosses are shown in light grey, second layer crosshairs are shown in black, the white background is the base layer of the silicon wafer.

A second PEB was performed to reveal and highlight key exposed features in the patterns of the second layers. PEB procedures are listed in Table 2.2. After the final PEB, it is important to verify that all features are aligned properly before proceeding to the feature development step. Improper alignment of features within the required error threshold would render the device mold useless.

Feature development varies depending on the type of photoresist used for device fabrication. Each type of photoresist has its own developer solution. ADEX photoresists require cyclohexanone, while SUEX photoresists require propylene glycol methyl ether acetate (PGMEA). For this reason, it is not recommended to combine multiple layers of ADEX and SUEX together on the same device mold.

To begin development, two clean glass bowls were obtained, one of which was filled with cyclohexanone developer solution. Wafer tweezers were used to submerge the wafer in a developer solution bath for 30-60 seconds. The wafer was then removed from the developer solution bath and gently shaken to remove residual solution. Next, the wafer was held at an angle above a waste container and sprayed with a squirt bottle containing Isopropyl Alcohol (IPA). The IPA stream was applied until white streak marks of unexposed photoresist ceased to appear. The wafer was gently shaken above the waste container to drain residual IPA, afterwards, the wafer was once again submerged in the developer solution bath for 30-60 seconds. The submerging, draining, and IPA wash steps were repeated until there were no more white streak marks washing off the wafer. Care was taken to avoid over-development of the wafer once the white streak marks were completely cleared. It is possible to partially delaminate exposed or crosslinked photoresist structures after submerging the wafer in developer solution for extended periods of time. It is also possible to partially delaminate exposed structures if excessive pressure is applied from the IPA wash bottle stream. Structures with larger surface area are more resistant to over-development, however, finer structures with dimensions under 100ums may undergo delamination in the event of over-exposure. After development, wafers were gently washed with deionized water (DI water) and dried using a nitrogen gun.

A hard bake procedure was performed to solidify all structures on the wafer and finalize the photoresist mold. The ADEX based neuronal coculture device mold was hard baked for 90 minutes at 150ºC. The oven was then turned off to allow the device to naturally cool down to room temperature. Device structures were less sensitive to deformation during the hard bake phase vs. the PEB phases. In some cases, hard baking was able to fix partial delamination of photoresist structures by making them more durable and less likely to break off.

After the device mold was prepared, a soft lithography technique was employed to develop PDMS replicas of the neuronal coculture device. PDMS solution was prepared by mixing a 10:1 ratio of base to curing agent. The solution was thoroughly mixed and placed in a degassing chamber to remove air bubbles. Device molds were formed into bowls using aluminum foil to contain the PDMS solution. After degassing, PDMS was poured into the device molds and once again placed in the degassing chamber for 1 hour. Next, the devices were placed in an oven and baked at 65⁰C for 3 hours to solidify the PDMS. It was found that devices could be baked even quicker at 100⁰C for ~35 minutes. After baking, the devices were left to rest overnight. The following day, the PDMS devices were peeled from their molds and cut to appropriate sizes. After cutting, devices were hole punched, cleaned, and plasma oxidized onto glass microscope slides in preparation for testing.
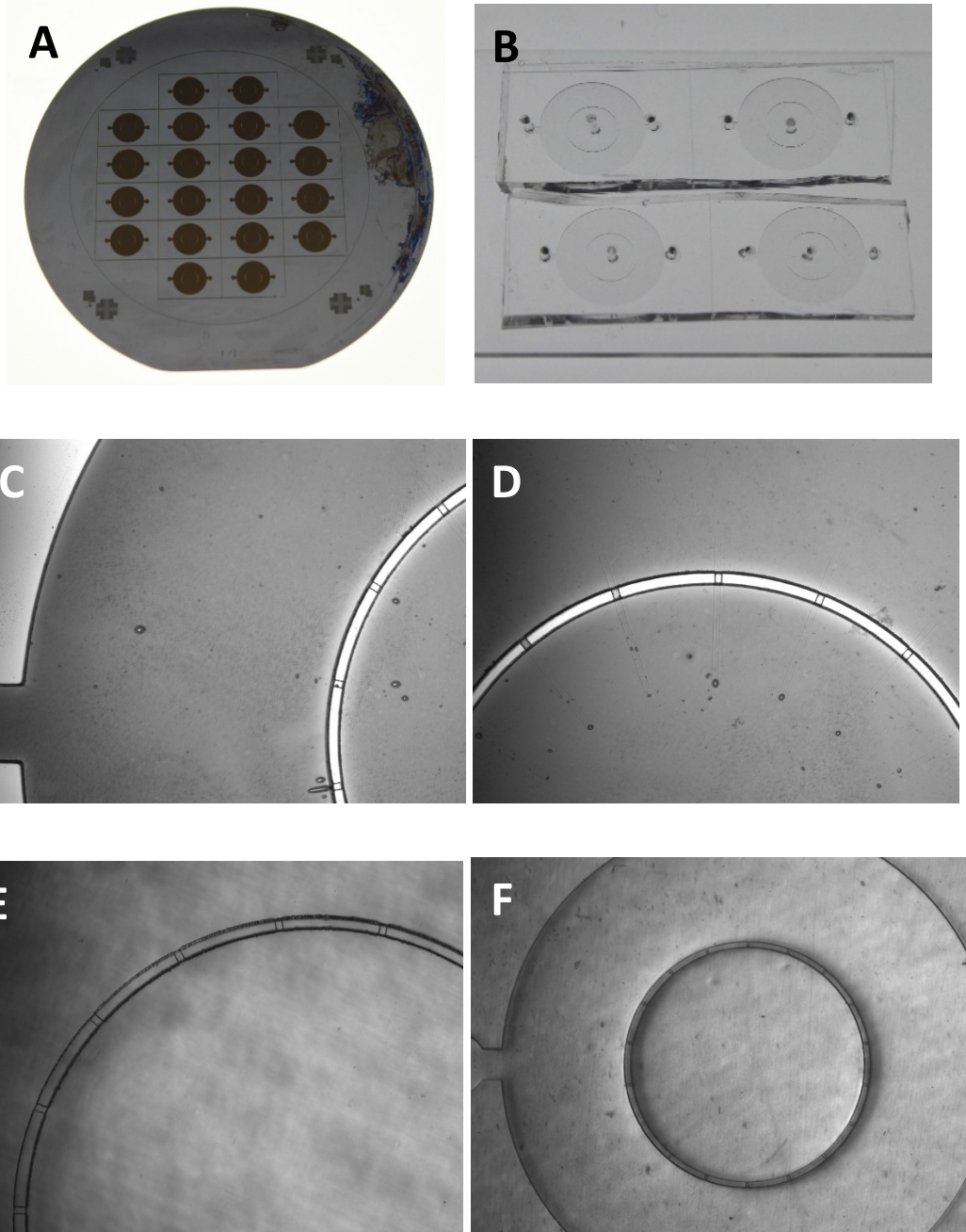
**Figure 2.5** Final neuronal coculture device assembly. (A) Master mold used for device fabrication, shown after final hardbake. (B) 4 units of the neuronal coculture device fabricated with PDMS, cut, hole punched, and plasma oxidized onto a glass slide. (C, D) Microscope images of a single device on the hard baked master mold. Microchannels are shown connecting the annular and central chambers. (E, F) Microscope images of a PDMS replica of the device.

## 2.4 Device Testing

After final fabrication, the neuronal coculture devices were handed off to Matt Blurton-Jones's lab for testing. Zahara Keulen, a graduate student in the lab, ran the coculture experiments. 10uL micropipettes were used to inject cells and media into the devices. Neuronal precursors were injected into the central chambers, while microglia were injected into the outer chambers. It was observed that no leakage occurred between chambers, indicating that the microchannels prevented free flow of neuronal precursors, and only allowed microglia to migrate inwards. After injection, microglia were able to migrate across the microchannels into the inner chamber overnight as shown in **Figure 2.6**. The device and microglia were imaged with a confocal microscope.
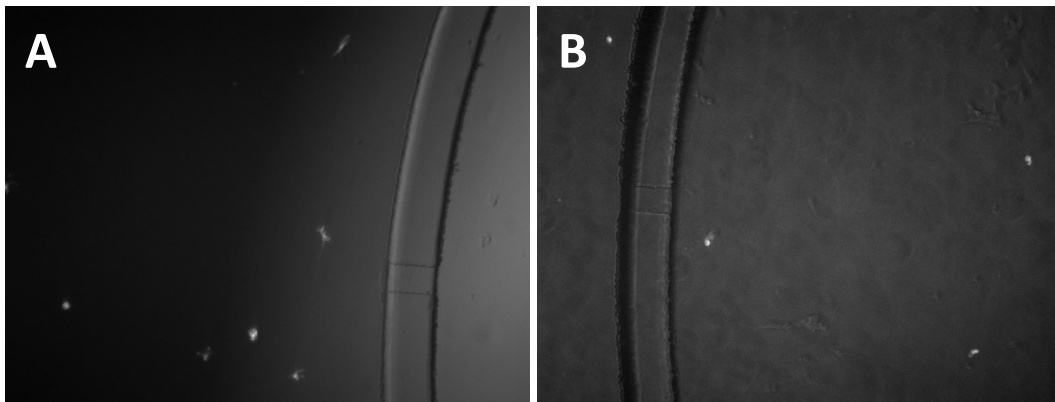


**Figure 2.6** Microglial migration from the annular chamber to the central chamber via microchannels. (A) Microglia, shown as white specs, were solely located in the annular chamber after initial injection into the device. (B) Microglia migrated overnight into the central chamber via the microchannels. Microchannels are shown as small rectangular struts linking the central and annular chambers.

Chapter 3: Hydrophoretic Filter Device Fabrication and Testing

3.1 <u>Background and Previous Work</u>

Hydrophoresis and hydrophoretic filtration has been heavily researched by Je-Kyun Park and Sungyung Choi in multiple works outlining the fabrication and use of such devices. Park and Choi's devices were primarily used to sort mammalian cells, blood cells, microparticles, and other microscale objects in the 8-20um diameter range [4,5,10,17,18]. Hydrophoresis, the method used to sort these particles, refers to the movement of suspended particles under the influence of microstructure-induced pressure fields. In this case, the microstructures refer to slanted obstacles and trenches located throughout the main channel of the devices used to sort these particles. Particle sorting refers to the separation of particles by size, with smaller particles often being sorted to one sidewall of the device while larger particles are sorted to the opposite sidewall. When particle suspensions containing a range of particle sizes are flown through the a hydrophoretic filter, a lateral distribution of particles can be observed in the outlet chamber.

Park and Choi have fabricated many variations of hydrophoretic filters, incorporating single sided trenches located along the bottom layer of the channels, and double trench designs where trenches are both suspended from the upper ceiling of the device and emerge from the base layer of the channel. Other obstacle variations include partial obstacles which do not span the entire width of the main channel. Partial obstacles are used for specific flow focusing such as the generation of spiral flow [18]. SU-8 lithography methods were consistently used in the creation of the master molds for these devices.

## 3.2 Design Considerations

The goal of this work was to fabricate and test a version of the hydrophoretic filter that would permit the sorting of larger scale particles up to 250um in diameter. The design chosen for our device was a single sided obstacle pattern, with trenches spanning the full width of the channel's ceiling layer.
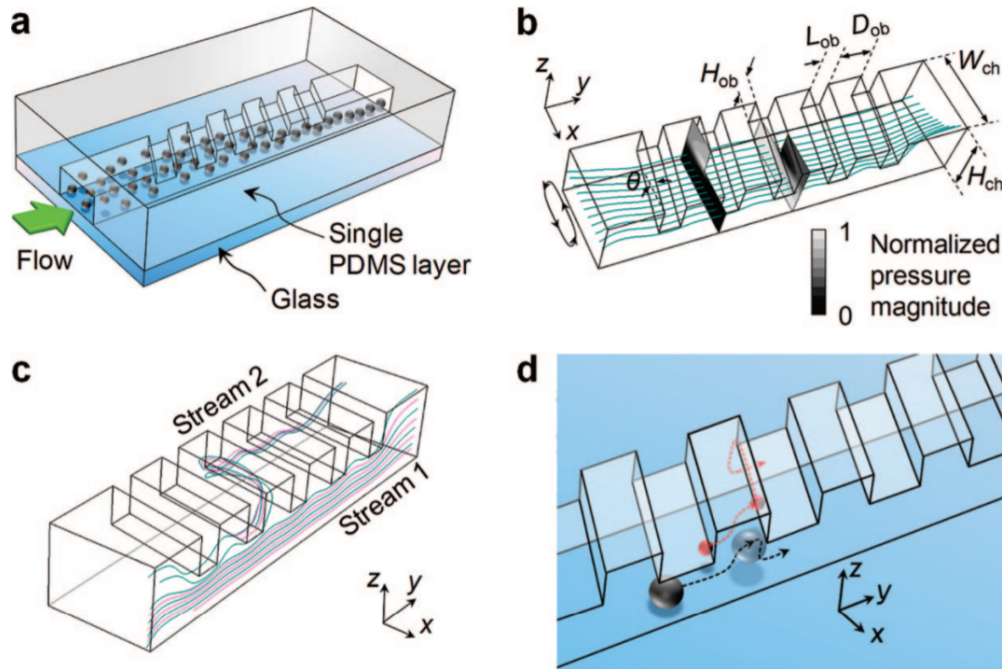


**Figure 3.1** Schematic of hydrophoretic filter demonstrating hydrophoretic particle separation [19]. (A) Schematic showing particles flowing through the device, encountering slanted obstacles, and being sorted towards the bottom sidewall. (B and C) Simulated streamlines and pressure gradients shown as fluid flows through the y-axis. Key channel dimensions are shown. $H_{ob}$ = height of obstacle, $L_{ob}$ = length of obstacle, $D_{ob}$ = distance between obstacles, $W_{ch}$ = width of channel, $H_{ch}$ = height of channel, $\theta$ = angle of obstacle slant. (D) Particles with diameters similar to the obstacle gap ($H_g = H_{ch} - H_{ob}$) will move upwards along the z-axis due to particle-wall interaction.

19

As shown in **Figure 3.1**, larger particles with diameters greater than ½ $H_g$ will steer closer to stream 1 towards the bottom sidewall, while particles with diameters less than ½ $H_g$ will steer towards the upper sidewall as part of stream 2. Our device dimensions are as follows: $H_{ob}$ = 300um, $L_{ob}$ = 200um, $D_{ob}$ = 100um, $W_{ch}$ = 800um, $H_{ch}$ = 550um, $\theta_1$ = 30⁰ for the 35 obstacles in the pre-channel, $\theta_2$ = 10⁰ for the 140 main channel obstacles. An inlet chamber measuring 2.6mm x 3mm was included for mixed particles to be injected into. Our master mold was used to create four units of the device. The upper and lower device copies contained rectangular outlet chambers measuring 5.4142mm x 3.6284mm. The two central copies of the device included a forked, 4-branch outlet, intended to capture streams of hydrophoretically sorted particles flowing out from the main channel. The four streams would ideally include particles sorted into diameter groups of <50um, 50um-100um, 100um-200um, and 200um-250um. The outlet chambers of these branched devices included upper and lower branches of 0.6414mm, and central branches of 0.9071mm. The 4 smaller branched outlet chambers were 2.366mm x 1.6414mm rectangles. Device dimensions and dark field photomasks were designed by Victor Yan, a graduate student of the Hui Lab. Photomasks were printed at CADart services with a minimum feature resolution of 8um.

Hydrophoresis Mask 1

Hydrophoresis Mask 2
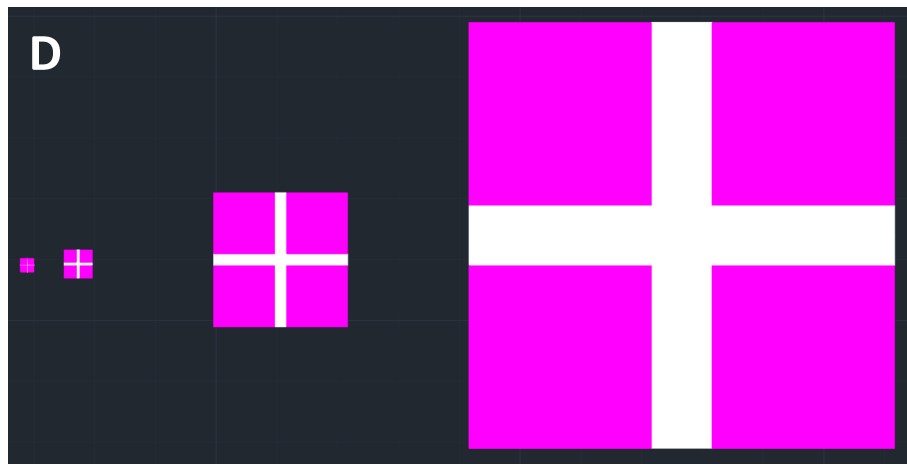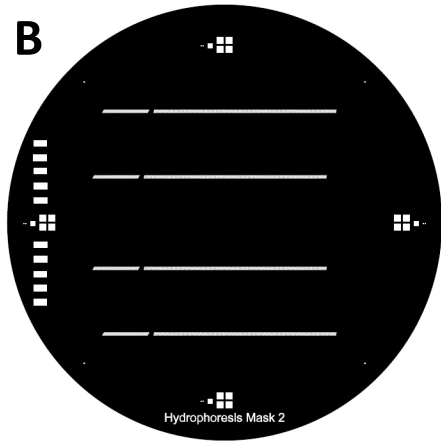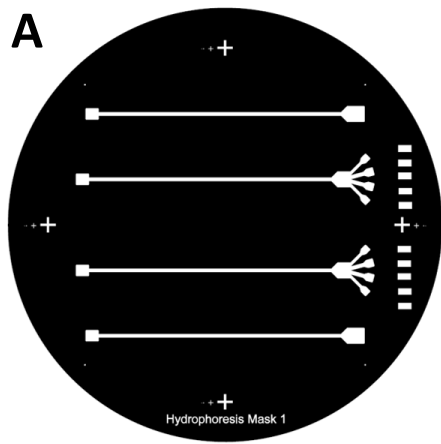
**Figure 3.2** Two photomasks used for the fabrication of the hydrophoretic filter. (A) Photomask design used for the first layer with 250um tall features. Design includes inlet chamber, outlet chamber, main channel, and 4 sets of cross alignment markers. The right edge of the photomask includes sets of 3mm x 50um lines used to test exposure durations. (B) Photomask design used for the second layer with 300um tall features. Design includes slanted obstacles, and 4 sets of crosshair alignment markers. The left edge of the photomask includes similar exposure test lines as the first photomask. (C) AutoCAD drawing of overlayed first- and second-layer features of the hydrophoretic filters. First layer features include the inlets, outlets, and main channel bodies shown in white. The second layer slanted obstacle features are shown in magenta. (D) AutoCAD drawing of overlayed first- and second-layer alignment markers from left edge of photomasks. First layer cross markers are shown in white while second layer crosshair markers are shown in magenta.

### 3.3 Device Fabrication

Fabrication of a master mold for the hydrophoretic filter device mostly followed the same procedure as the neuronal coculture device with some variable alterations. Firstly, exposure duration lengths had to be increased due to thicker photoresists being used to build the mold. Exposure durations are shown in Table 3.1. Optimal exposure duration was determined by performing a sweep of exposure duration tests using the 3mm x 50um test features incorporated into each photomask.

| Device Layers | Photoresist Height | Exposure Duration |
|---|---|---|
| Layer 1 | 250um (SUEX) | 4 minutes |
| Layer 2 | 300um (SUEX) | 4 minutes and 30 seconds |

**Table 3.1** UV exposure durations for optimized feature development of the hydrophoretic filter

When performing the first layer PEB on the Hydrophoresis device mold, initial trials were conducted using the same PEB procedure and parameters as the neuronal coculture device. However, it soon became apparent that the PEB procedure had to be drastically modified for the thicker SUEX layers due to properly highlight their feature patterns. Two separate sets of PEB parameters were initially tested on the first 250um layer of the Hydrophoresis device mold. The tested parameters included UV exposure duration, baking temperature(s), and bake durations at set temperatures.

| Trial Procedures | Exposure Duration | PEB Procedure |
|---|---|---|
| Trial 1 | 3 minutes | 1) Pre-heat oven to 85ºC<br>2) Bake wafer for 30 mins at 85ºC<br>3) Turn off oven and cool wafer inside for 2-3 hours until oven reaches 40ºC |
| Trial 2 | 3 minutes and 30seconds | 1) Pre-heat oven to 95ºC<br>2) Bake wafer for 30 mins at 95ºC<br>3) Turn off oven and cool wafer inside for 2-3 hours until oven reaches 40ºC |
| Trial 3 | 4 minutes | 1) Pre-heat oven to 50ºC<br>2) Bake wafer for 5 minutes at 50ºC<br>3) Set oven to 65ºC and bake wafer for 10 minutes<br>4) Set oven to 80ºC and bake wafer for 10 minutes<br>5) Set oven to 85ºC and bake wafer for 1 hour<br>6) Set oven to 65ºC and bake wafer for 1 hour<br>7) Set oven to 45ºC and bake wafer for 1 hour<br>8) Turn off oven, wait 1 hour for oven to reach 30ºC, then remove the wafer |

**Table 3.2** Various parameters tested to achieve optimal PEB conditions for 250um SUEX photoresist layer.
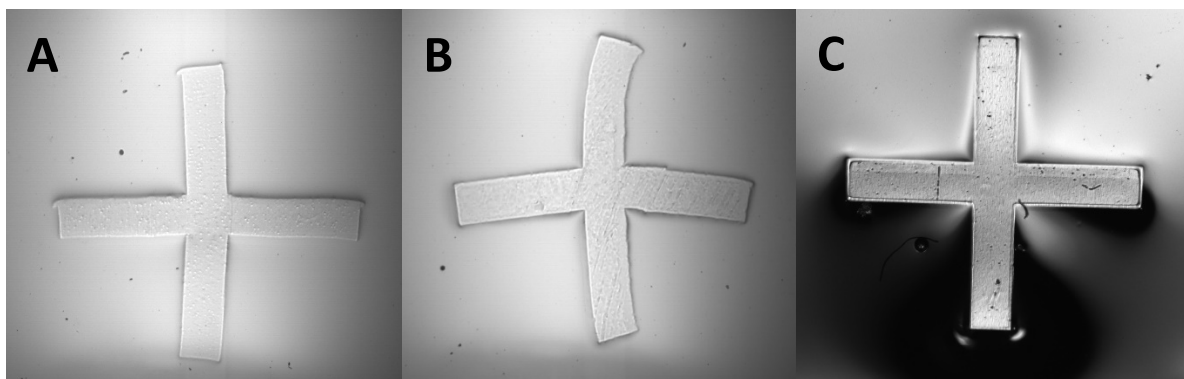
**Figure 3.3** Alignment marker features imaged after each PEB trial shown in **Table 3.2**. (A, B) Trials 1 and 2 resulted in misshapen alignment marker due to insufficient UV exposure, rapid temperature fluctuations, and inadequate cooling during the PEBs. (C) Trial 3's PEB procedure included more gradual temperature ramp up and cool down steps, resulting in well defined alignment markers and other design features.

A recurring issue in the first two PEB optimization trials was feature deformation that occurred because of rapid temperature fluctuations during the PEB. If a wafer was not given enough time to cool to room temperature after a PEB, or if temperatures were changed too quickly during the PEB, extremity features such as alignment markers would deform into pitchfork shaped patterns, rendering them useless for accurate alignment. In Trial 3, a unique SUEX PEB procedure was employed, whereby the oven used for baking was preheated to 50°C, the wafer was inserted into the oven and the temperature was gradually increased to 85°C over 30 mins. After reaching 85°C, the wafer was baked for 1 hour, then cooled to room temperature at a rate of 20°C/hr [20]. The same PEB procedure was used for both layers of the hydrophoretic filter mold to much success. It should be noted that the exposure duration tests used to determine the optimal SUEX layer exposure durations presented in **Table 3.1** could only be performed after

the optimal PEB procedure was determined, hence why the exposure durations vary in the trials presented in **Table 3.2**.

To create the second mold layer, a 300um tall, 96mm diameter SUEX photoresist was laminated onto the wafer at a speed of 3 at 70⁰C. Care was taken to properly align the two layers to prevent edge fracturing of misaligned and overhanging sections of the photoresist sheet. With a diameter of 96mm, the second photoresist layer completely covered the first layer features including the alignment markers. For this reason, smaller alignment markers with cross spoke features less than 30um were less visible through the semi-transparent photoresist.
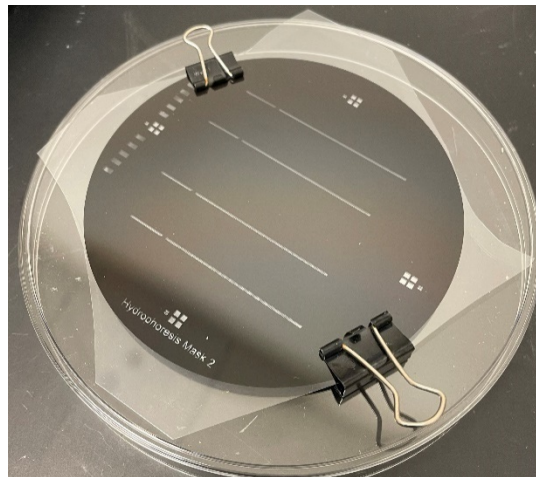


**Figure 3.4** Multi-Layer alignment assembly used for second layer exposure of the hydrophoretic filter device

The device alignment assembly is shown in **Figure 3.4**, alignment markers were positioned following the same technique shown in **Figure 2.4.** Second layer exposure was performed for 4 minutes, and 30 seconds as shown in **Table 3.1.** A second PEB was performed following the new SUEX PEB procedure. Feature development was conducted in the same

manner as the neuronal coculture device procedure, except for substituting PGMEA as the SUEX developer solution. An example of overdevelopment is shown in **Figure 3.5**.
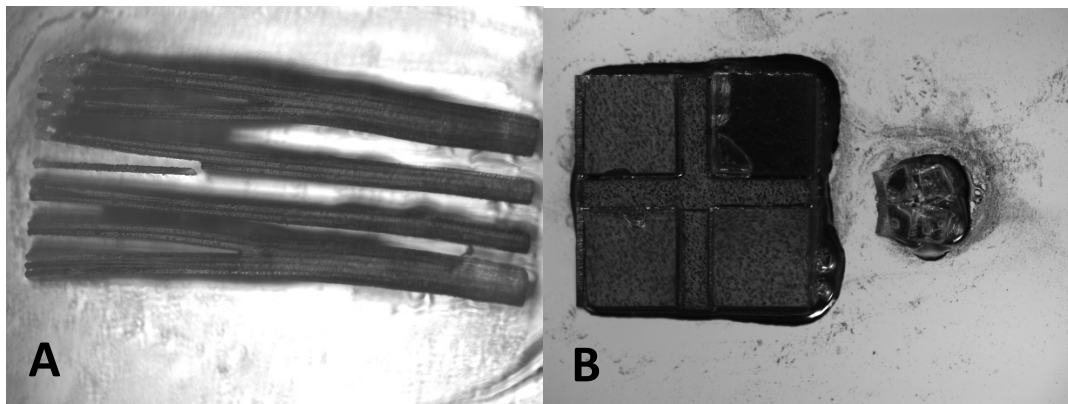


**Figure 3.5** Partial destruction of mold features due to overdevelopment. (A) Exposure test lines shown bent and angled. (B) Partial delamination and bending of the rightmost alignment marker. Features imaged after hard bake step.

After feature development, a hard bake was performed to solidify all structures on the wafer and finalize the photoresist mold. The SUEX device mold was hard baked for 1 hour at 125⁰C. The oven was then turned off to allow the device to naturally cool down to room temperature. Hard baking was able to fix partial delamination of photoresist structures by making them more durable and less likely to break off. After hard baking, the same soft lithography procedure was used to create PDMS copies of the hydrophoretic filter.
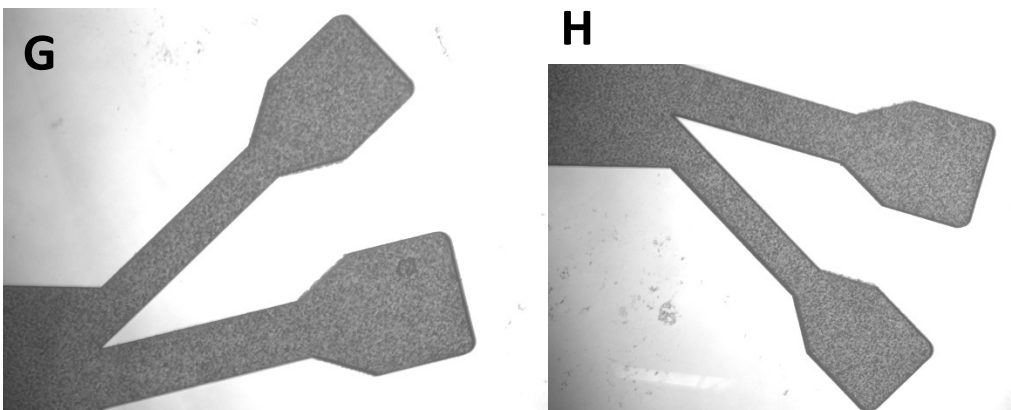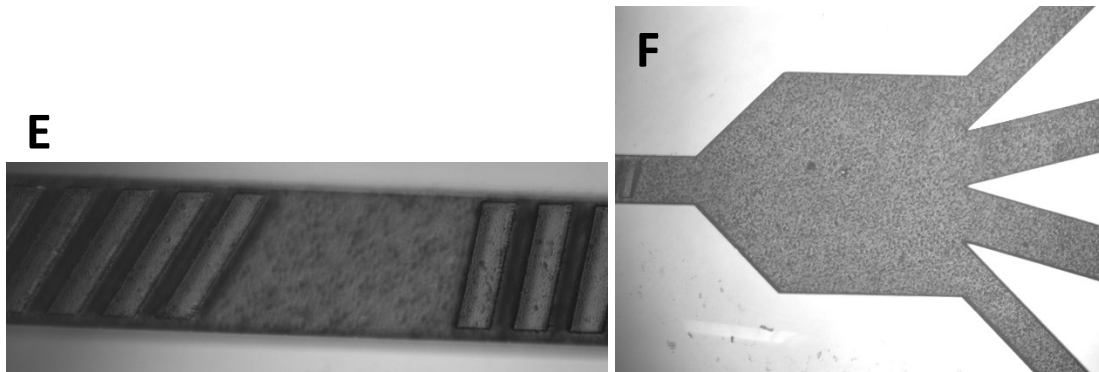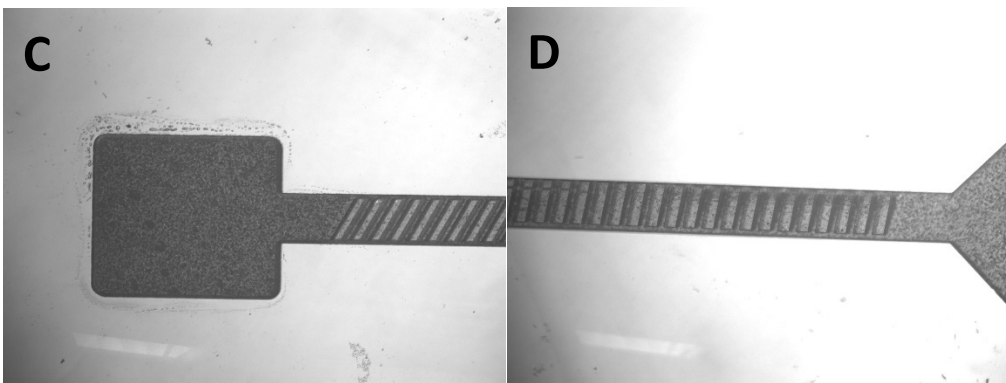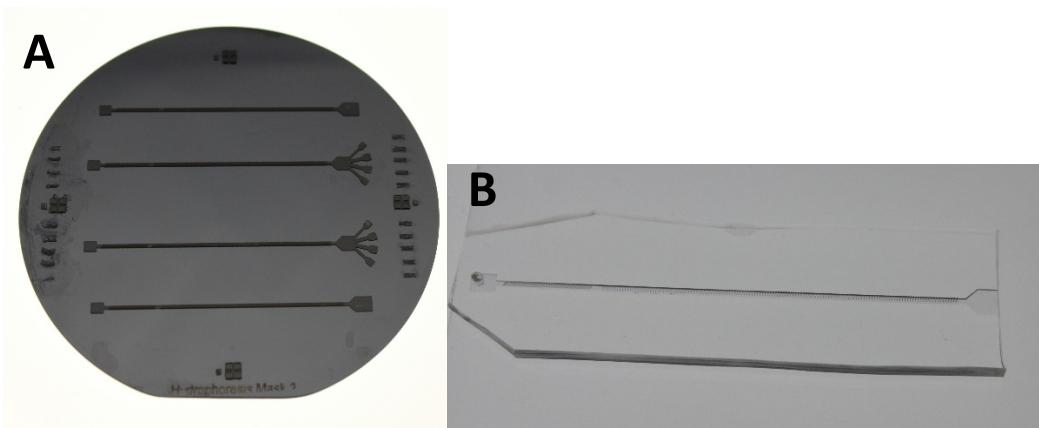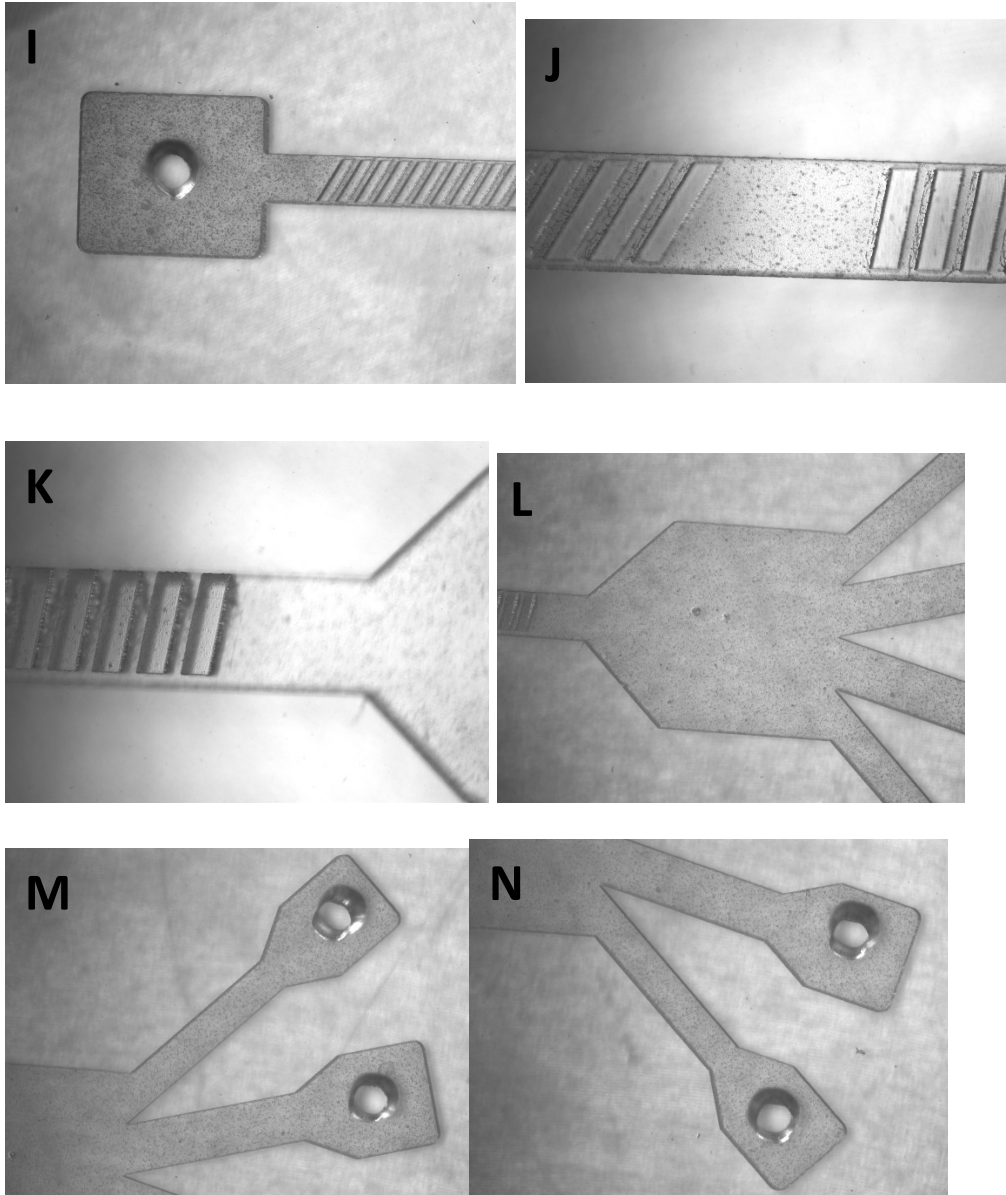
**Figure 3.6** Final hydrophoretic filter device assembly. (A) Master mold used for device fabrication, shown after final hardbake. (B) A single unit of the hydrophoretic filter device fabricated with PDMS, cut, hole punched, and plasma oxidized onto a glass slide. This variation of the device has had its branched outlets cut off. (C, D, E, F, G, H) Microscope images of the hard baked master mold used to fabricate the hydrophoretic filter. (I, J, K, L, M, N) Microscope images of a PDMS replica of the hydrophoretic filter with hole punched inlets and outlets.

3.4 Device Testing

After the fabrication of PDMS copies of the hydrophoretic filter, the device's sorting

capabilities and flow mechanics were tested. A mixed set of polystyrene microcarriers ranging

from 125-212 microns in diameter were obtained to test the hydrophoretic sorting. Based on the

particles' diameters, they should be laterally sorted towards the middle-lower half of the outlet

chamber. A bead solution was prepared by suspending polystyrene microcarrier beads at 0.12%

(v/v) in a 0.2% Tween 20 solution, care was taken to gently vortex the solution to minimize

bubble formation [18]. A separate 0.2% Tween 20 solution was prepared for use as a primer.

Bead solution was then drawn into a 10mL syringe fitted with a yellow 20-gauge needle tip

(diameter of 0.9mm). The syringe was mounted onto a syringe pump (Harvard Apparatus, Pico

Plus) calibrated for a 14.5mm diameter 10mL syringe. Clear PTFE (Polytetrafluoroethylene)

tubing with an inside diameter (ID) of 0.8mm and an outside diameter (OD) of 1.2mm was used

to connect the syringe needle to the inlet chamber of the hydrophoretic filter. All holes in the

PDMS device were punched with a 1.2mm diameter hole puncher (TedPella). Four additional

pieces of tubing were connected to the hole punched branched outlet chambers of the

hydrophoretic filter and drawn into four separate 15mL conical tubes used as collection

chambers for the outflowing beads and liquid. The device assembly is shown in **Figure 3.7**.
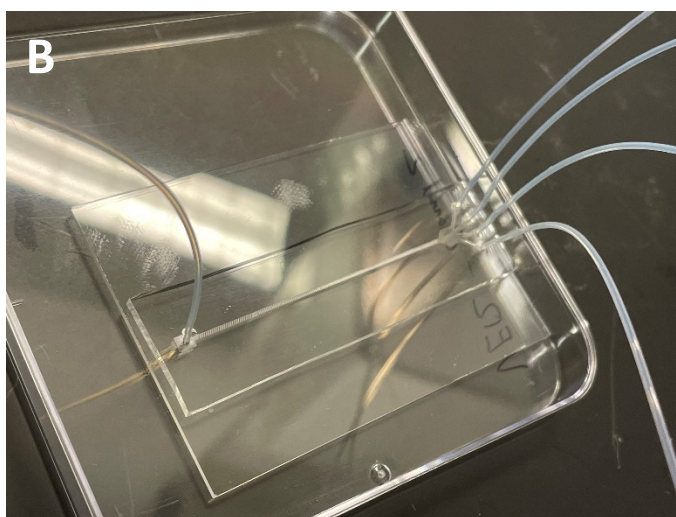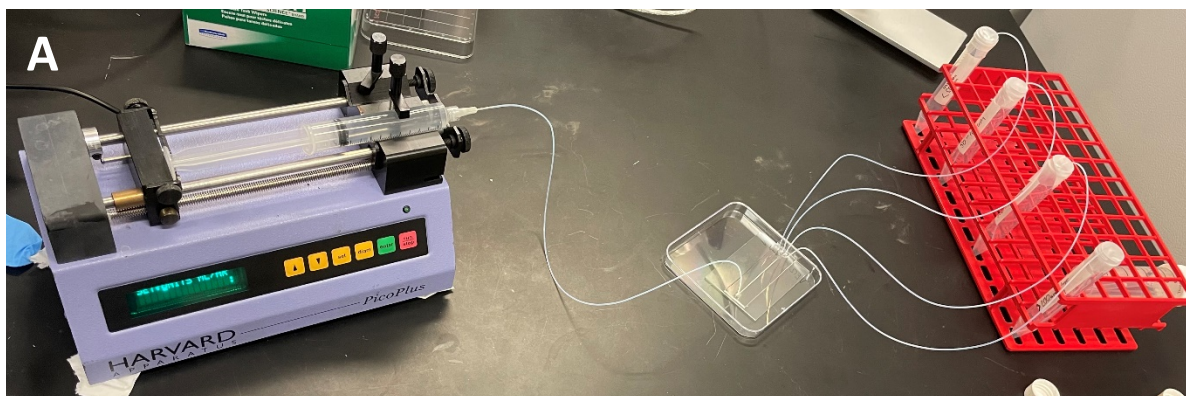
**Figure 3.7** Early testing assembly used for passaging of bead solution through a PDMS hydrophoretic filter device. (A) Full device assembly including syringe pump, syringe, inlet tubing, PDMS device, outlet tubes, and conical collection tubes. (B) PDMS hydrophoretic filter device with tubing connected to the inlet and four outlet chambers.

Early iterations of the testing assembly used different hole punch, needle, and tubing diameters. A 20G needle, 0.8mm ID tubing, and 1.2mm diameter hole punches located close to the outer edges of the inlet/outlet chambers were later used to decrease clogging of beads as they passed through the tubing. A USB microscope was positioned above the PDMS device and focused onto the outlet chamber to capture footage of beads being laterally sorted. The 4 collection tubes used for the device were labeled "<50um beads", "50um-100um beads",

"100um-200um beads", and ">200um beads" from top to bottom. Theoretically, most beads should have been sorted to the third size category, with a few outliers going towards the fourth size category, however, flow testing soon revealed issues with drainage that would counteract any hydrophoretic sorting that occurred.

In the first rounds of bead sorting trials, the syringe pump was set to various flow rates between 0.1mL/hr and 9mL/hr as beads were gradually pumped through the device. It was quickly determined that a Tween 20 primer solution was not necessary to operate the device, and the act of switching the tubing connected to the device inlet between a syringe with bead solution and a syringe with primer solution introduced bubbles into the device which hindered hydrophoresis. When working with slower flow rates, it became necessary to frequently agitate or flip the syringe from one side to another to resuspend the microcarriers, as their density would cause them to gradually sink to the bottom of the syringe and not get properly passaged. On multiple occasions when high volumes of the bead solution were pumped through the device for a long period of time, it was observed that the four collection tubes would collect disproportionate amounts of solution. Often times, all fluid outflow would be directed to a single outlet branch. Many variables were adjusted to see what contributed to this phenomenon, including flow rate, height of the PDMS device relative to the pump, height of the collection tubes relative to the PDMS device, hole punch diameter, tubing diameter, needle diameter, bead concentration, and outlet tube length. After many inconclusive tests, a new test was conducted where 10mL of DI water was forcefully hand pumped through the device assembly at an approximate rate of 5mL/s. After each trial, the amount of water in each of the four 15mL conical tubes was recorded to obtain a rough estimate of the disproportionate outflow ratio of the device. The test results are shown in **Table 3.3.** The conical tubes are referred to as C1-C4 based

on their lateral position from top to bottom, with C1 corresponding to the "<50um beads" tube and C4 corresponding to the ">200um beads" tube.

| Trial # | C1 mL | C2 mL | C3 mL | C4 mL | C1 % | C2% | C3% | C4% |
|---|---|---|---|---|---|---|---|---|
| 1 | 1.5 | 3.0 | 3.5 | 1.5 | 0.158 | 0.316 | 0.368 | 0.158 |
| 2 | 2.0 | 3.5 | 4.0 | 2.0 | 0.174 | 0.304 | 0.348 | 0.174 |
| 3 | 1.5 | 3.0 | 3.5 | 1.5 | 0.158 | 0.316 | 0.368 | 0.158 |
| 4 | 2.0 | 3.0 | 3.5 | 2.0 | 0.190 | 0.286 | 0.333 | 0.190 |
| 5 | 2.0 | 3.0 | 3.5 | 2.0 | 0.190 | 0.286 | 0.333 | 0.190 |
| 6 | 1.5 | 3.0 | 3.5 | 2.0 | 0.150 | 0.300 | 0.350 | 0.200 |
| 7 | 1.0 | 3.0 | 3.5 | 1.5 | 0.111 | 0.333 | 0.389 | 0.167 |
| 8 | 1.5 | 3.0 | 3.5 | 2.0 | 0.150 | 0.300 | 0.350 | 0.200 |
| 9 | 1.5 | 3.0 | 3.5 | 1.5 | 0.158 | 0.316 | 0.368 | 0.158 |
| 10 | 1.0 | 3.0 | 3.5 | 1.5 | 0.111 | 0.333 | 0.389 | 0.167 |
| Average | 1.6 | 3.1 | 3.6 | 1.8 | 0.155 | 0.309 | 0.360 | 0.176 |

**Table 3.3** Results of hand pumped fluid tests on hydrophoretic filtration device. Distribution of 10mL of water between four 15mL conical tubes is shown. Columns 2-5 show total volume of liquid in each tube. Columns 6-9 show percentage of total water that was pumped to each tube.

The hand pump trials confirmed that water was disproportionately flowing between the conical tubes at approximately a 1:2:2:1 ratio. This outcome was likely due to the upper and lower branches of the device outlet being designed with narrower 0.6414mm channels while the two central branches were designed with thicker 0.9071mm branches. To counteract the uneven geometry of the outlet chamber, a new reverse flow pump design was tested. In these trials, four syringes were each labelled in correspondence to the four conical tube bead size categories. The four syringes were connected to a reverse syringe pump which would pull bead solution through the four outlet branches of the device at an even flow rate. While initial tests with DI water showed that this configuration would be possible for even outflow, tests with bead solutions revealed a new issue. Even if beads were hydrophoretically sorted through the main channel of

the device, they were observed to get sucked up by the bottom three branching outlet channels at random due to the pulling force of the outlet branches disrupting the hydrophoretic sorting that had occurred. Theoretically, only the bottom two branch channels (100um-200um and >200um) should receive the 125um-212um beads, but as shown in **Figure 3.8**, it was possible for beads to get sucked into the 50um-100um outlet branch as well.
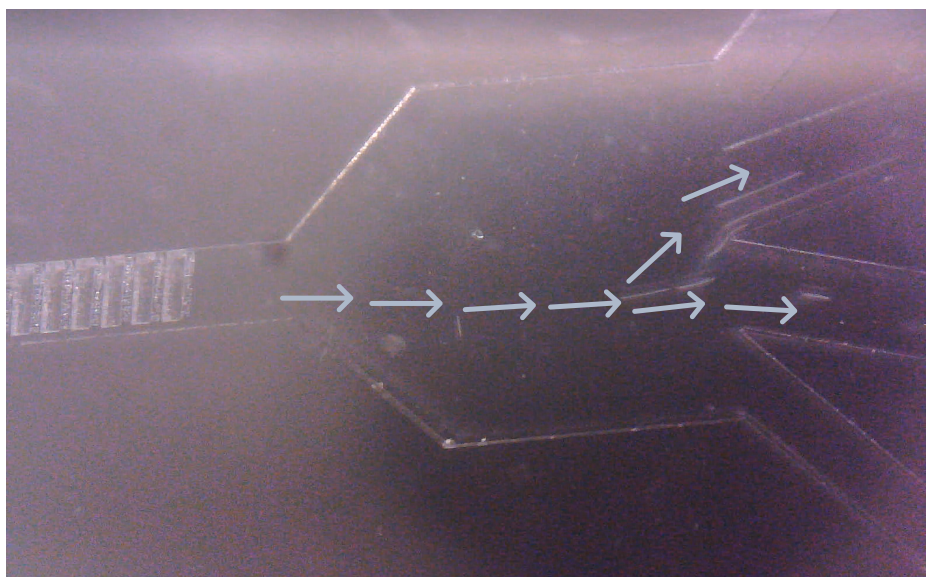


**Figure 3.8** Passaging of beads in a 4 pump, reverse flow configuration. A stream of beads is pulled to the lower half of the outlet chamber, only to be randomly split between the two middle outlet branches.

To fix these various flow issues, the decision was made to revert to forward flow passaging of beads while cutting off the forked ends of each new hydrophoretic filter PDMS device that was fabricated, leaving only an open edge slit for bead solution to spill out of, as shown in **Figure 3.6b**. Despite the open outflow of bead solution, the hydrophoretic sorting process would no longer be interrupted with this configuration, and bead collection would become a problem deferred for future work.

Bead sorting tests were conducted on the edge-cut variant of the hydrophoretic filter device. Beads were sorted at 1mL/hr, 5mL/hr, and 10mL/hr at high and low concentrations. High concentrations of beads were attained by positioning the syringe pump on its side, allowing the syringe tip to face downwards so all beads would sink near the syringe tip and be flown through the device at high frequency. Passaging of high concentrations of beads at flow rates above 10mL/hr resulted in occasional flaring and consistent straight-shooting of beads down the middle of the outlet chamber. The flaring behavior would result in beads being incorrectly displaced to the top half of the outlet chamber, where beads below 100um in diameter would flow, confirming that hydrophoresis was not occurring under these conditions. Passaging of low concentrations of beads with flow rates at or below 5mL/hr resulted in lateral displacement of beads to the lower half of the outlet chamber. Overall, hydrophoretic sorting behavior was observed to occur at a maximum flow rate of 5mL/hr with a mid to low concentration of 125-212um diameter beads flowing through the device. The next step for testing the device was to confirm if hydrophoretic sorting of smaller particles (<100um diameter) would occur in similar conditions.
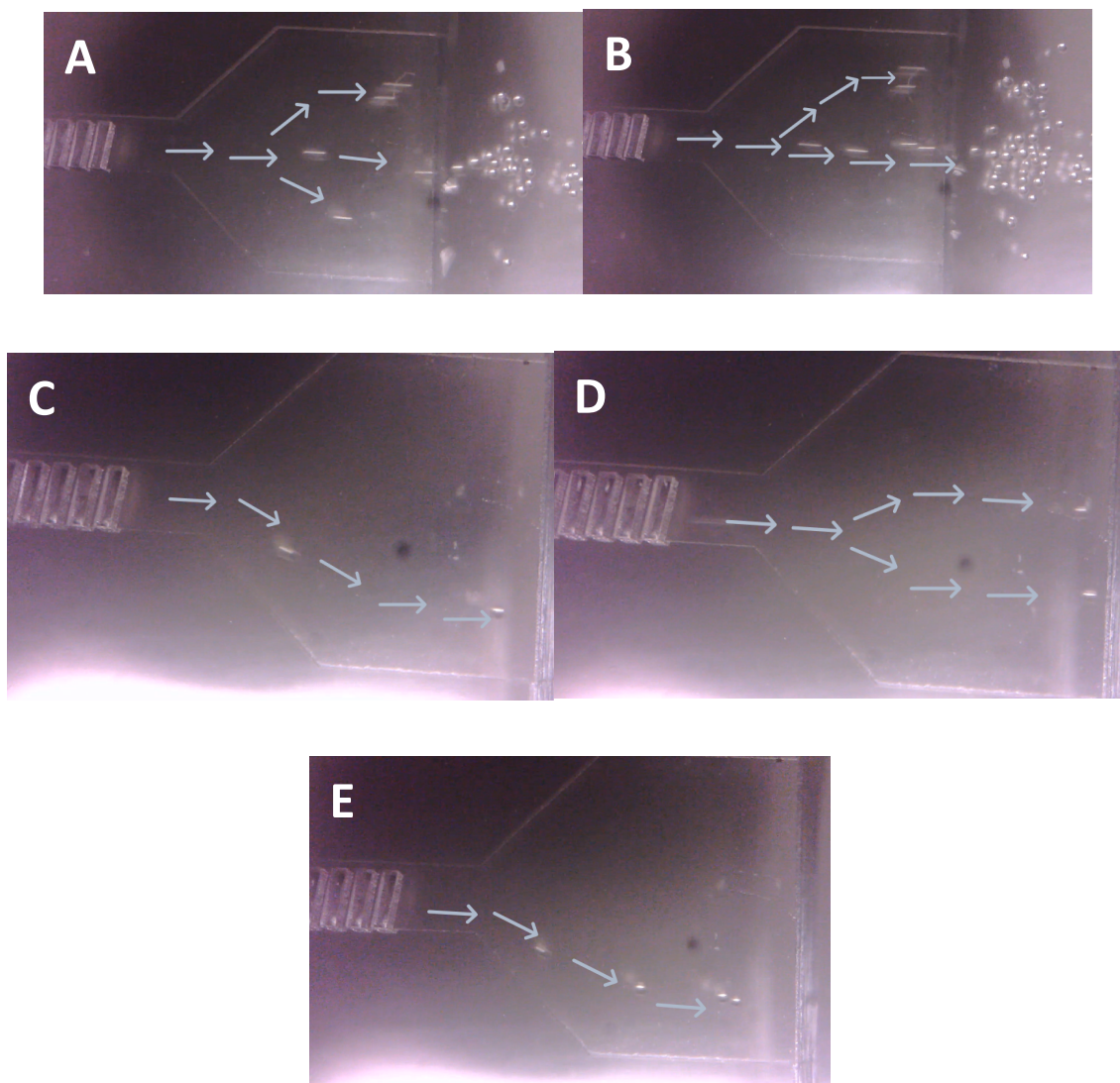
**Figure 3.9** Bead sorting tests with edge-cut hydrophoretic filter device. Arrows were added to figures to depict flow currents. (A, B) High concentrations of beads sorted at 10mL/hr through the hydrophoretic filter result in flaring behaviors and improper lateral displacement of beads. (C, D, E) Low concentrations of beads sorted at 5mL/hr through the hydrophoretic filter result in proper lateral distribution of beads to the middle and lower regions of the outlet chamber.

Sorting tests were conducted with murine pancreatic cancer cells to test the sorting capabilities of the hydrophoretic filter on smaller particles. With the help of Alica Beutel from

Dr. Chris Halbrook's lab, pancreatic cancer cells derived from a genetically engineered mouse model which faithfully recapitulates human pancreatic ductal adenocarcinoma were cultured, suspended in media, diluted with phosphate buffered saline (PBS) and a fluorescence-activated cell sorting (FACS) buffer, and placed through a series of mesh sieves to obtain various size categories of cell clusters and single cells. Cells were initially filtered through a 100um mesh sieve to remove any clusters above 100um in diameter, obtaining a set of cell solution labeled "<100um cells". Afterwards, cells would be further filtered through a 40um mesh to create a "<40um cells" solution, in the hopes of seeing a higher concentration of single cells measured to be roughly 20-30um in diameter. Despite mesh filtration being conducted right before the hydrophoretic filter tests, it should be noted that cells were still capable of attaching to each other to form larger clusters, in rare cases possibly exceeding 100um diameters. Cells sorting trials were recorded with a USB microscope and cell sizes were measured with ImageJ analysis.

The "<100um cells" media solution was tested in the first round of trials. Cells were flown through the device at rates of 1mL/hr, 5mL/hr, and 9mL/hr. For all trials, cells were shown flowing throughout the entire span of the outlet chamber, not concentrated to a single area in the upper half of the chamber as they theoretically should be, however, the "<100um cells", formed a somewhat concentrated stream of cells flowing to the top quarter of the outlet chamber where <50um cells would theoretically be sorted to. The occurrence of this upper stream was inconsistent, as it initially appeared when sorting at 1mL/hr **Figure 3.10a**, containing average cell cluster sizes of 50-80um diameters in the upper stream. Sorting at 5mL/hr caused cells to be randomly distributed throughout the outlet chamber with no clear upper stream. Sorting at 9mL/hr **Figure 3.10b** once again cause the upper stream to appear with average cell sizes of 20-50um diameters.

The "<40um cells" solution was tested in the second round of trials, at the 5mL/hr and 9mL/hr flow rates. Once again, cells were observed flowing throughout the entire outer chamber in non-concentrated manner. At 5mL/hr, cells did not form a clear upper stream, however, large clusters could be seen flowing through the lower half of the outlet chamber. The upper section of the outlet chamber contained cells no larger than 50um in diameter, while the lower portion mostly contained cells between 50-100um. At 9mL/hr, cells vaguely formed upper and lower streams with some cell clusters floating through the center of the outlet chamber. All cells in the upper stream were <50um in diameter. Overall, these results were not clear enough to indicate that successful hydrophoretic filtration was taking place, and more testing would need to be conducted in future work.
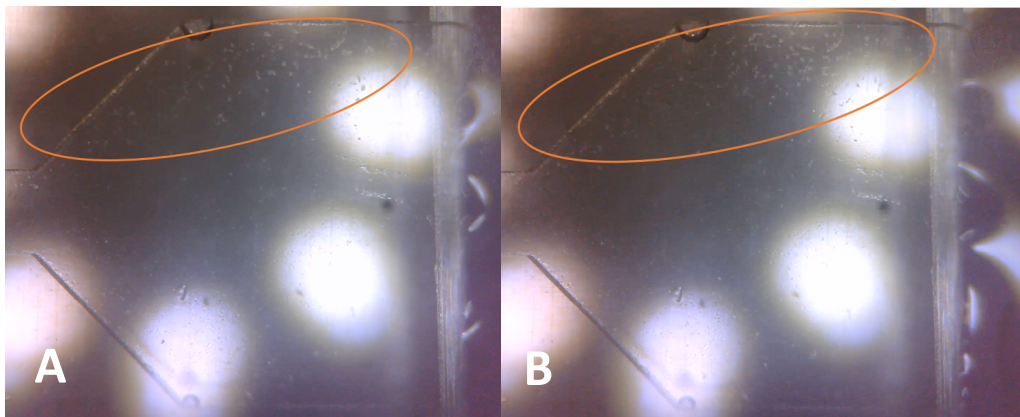


**Figure 3.10** Murine pancreatic cancer cells forming concentrated upper streams as they are sorted through the hydrophoretic filter. (A) Cells sorted at 1mL/hr. (B) Cells sorted at 9mL/hr.

Chapter 4: Organoid Droplet Generator Testing

4.1 Background

The designing and fabrication of the hydrophoretic filter device was one part of a joint project between the University of California, Irvine and the University of Illinois, Chicago. The joint work was funded by the Center of Advanced Design and Integrating of Microfluidics (CADMIM) as project number Y8-004: "Reproducible Generation and Passaging of Patient-Derived Cancer Organoids". The project goal was to create a method for the generation of patient-derived cancer organoids for the express purpose of testing drug treatment therapies for pancreatic cancer in an expedient manner, preventing a patient's cancer from developing into late stages. As an alternative to culturing uniform groups of cells from single cell samples, cancerous tissue could be gathered from a patient, sorted through the hydrophoretic filter into uniform size categories, and developed into similar sized organoids for drug screening. It is imperative that similar sized cell clusters or tissues are used in each organoid to eliminate the attribution of a successful or unsuccessful drug treatment option to the size or amount of cancerous tissue in the organoids. After sorting cancer cell clusters into similar sized categories, a droplet generation device would be used create evenly sized droplets from cells encapsulated in Matrigel droplets. Matrigel is gelatinous protein mixture derived from mouse tumor cells used as a basement membrane matrix used to promote cell differentiation [11, 21]. The application of this organoid generation technique for drug screening would improve the accuracy of organoid models.

<u>4.2 Device Design</u>

A droplet generator device was designed by Amirreza Gahznavi and 3D printed by Adam Szmelter of Dr. David Eddington's Lab at the University of Illinois, Chicago [22]. The device uses an oil-surfactant mixture pumped at a high flow rate to pinch beads off a stream of Matrigel. The device contains 3 inlets of which only two, B and C, were used. Matrigel, or Matrigel mixed with cells, were flown through inlet B, while the oil mixture was flown through inlet C. Outlet D was used for Matrigel droplets and excess oil to be extruded as shown in **Figure 4.1**. In this work, inlet A was sealed to prevent backflow. Cultrex Basement Membrane Extract was used as a Matrigel alternative. The oil-surfactant mixture was prepared by mixing Novec 7500 Hydrofluoroether (HFE) with Perfluoropolyether (PFPE) oil at a ratio of 11.25mL of Novec to 1.8g of PFPE.
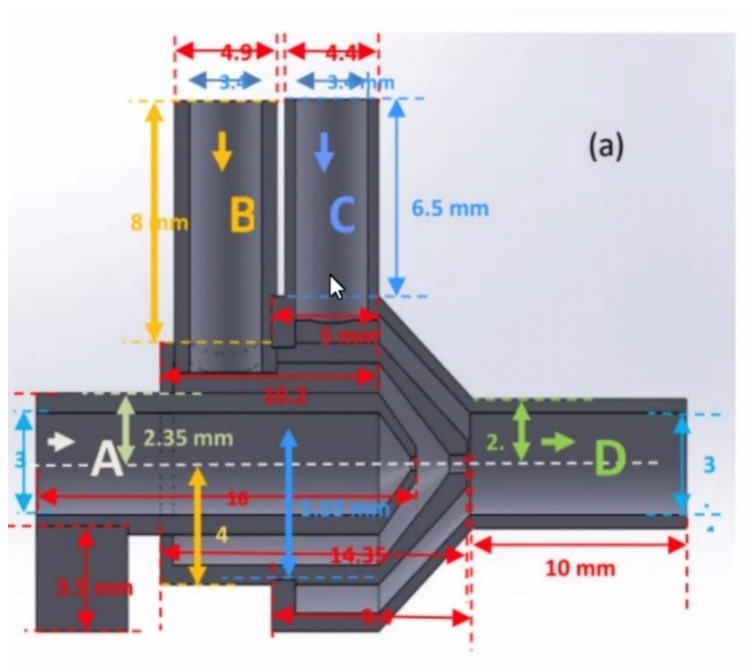


**Figure 4.1** Conceptual view of the droplet generator head. Figure and device were designed by Amirreza Gahznavi.

4.3 Device Testing

The droplet generator device was initially tested with no cells mixed into the Matrigel, and later with cells mixed into the Matrigel. Non-cell droplet tests were initially used to calibrate the device, finding the optimum flow rates needed for pumping the oil mixture and the Matrigel. For the device to work, oil had to be pumped at 10 times the rate of the Matrigel. Adam had seen success with flow rates of 1mL/min for the oil and 0.1mL/min for the Matrigel. Unfortunately, the syringe pumps (Harvard Apparatus, Pico Plus) available for this experiment had a maximum flow rate of 0.15mL/min. Thus, in early trials, the flow rate ratio was maintained by using 0.15mL/min for the oil and 0.015mL/min for the Matrigel.

The experimental set up is shown in **Figure 4.2**. To start, Matrigel and the oil mixture were drawn into separate 3mL syringes and attached to two syringe pumps placed on elevated platforms. The syringe pumps were calibrated to the 8.6mm diameter of the 3mL syringes. Each syringe was fitted with a round ended 14G olive green needle and connected to 15G (1.8mm ID) tubing. Tubing was then connected to the appropriate inlet chambers and outlet chamber of the generator head. The entrance to chamber A and the connection points of all tubing were secured with super glue to create a tight seal and prevent leaking. After the super glue had hardened, the oil chamber and Matrigel chamber were primed respectively. A conical tube was then positioned under the suspended end of the outlet chamber tubing to collect the falling Matrigel droplets and extruded oil. The conical tube was filled with warm water set to 37°C to gel the Matrigel droplets and prevent them from merging with each other after extrusion. Excess extruded oil would form a layer atop the warm water, and Matrigel beads would sink to the edge of the oil-water interface. To extract the beads, a pipet would be used to remove as much of the oil and water as possible, and the beads would be moved to a separate container.
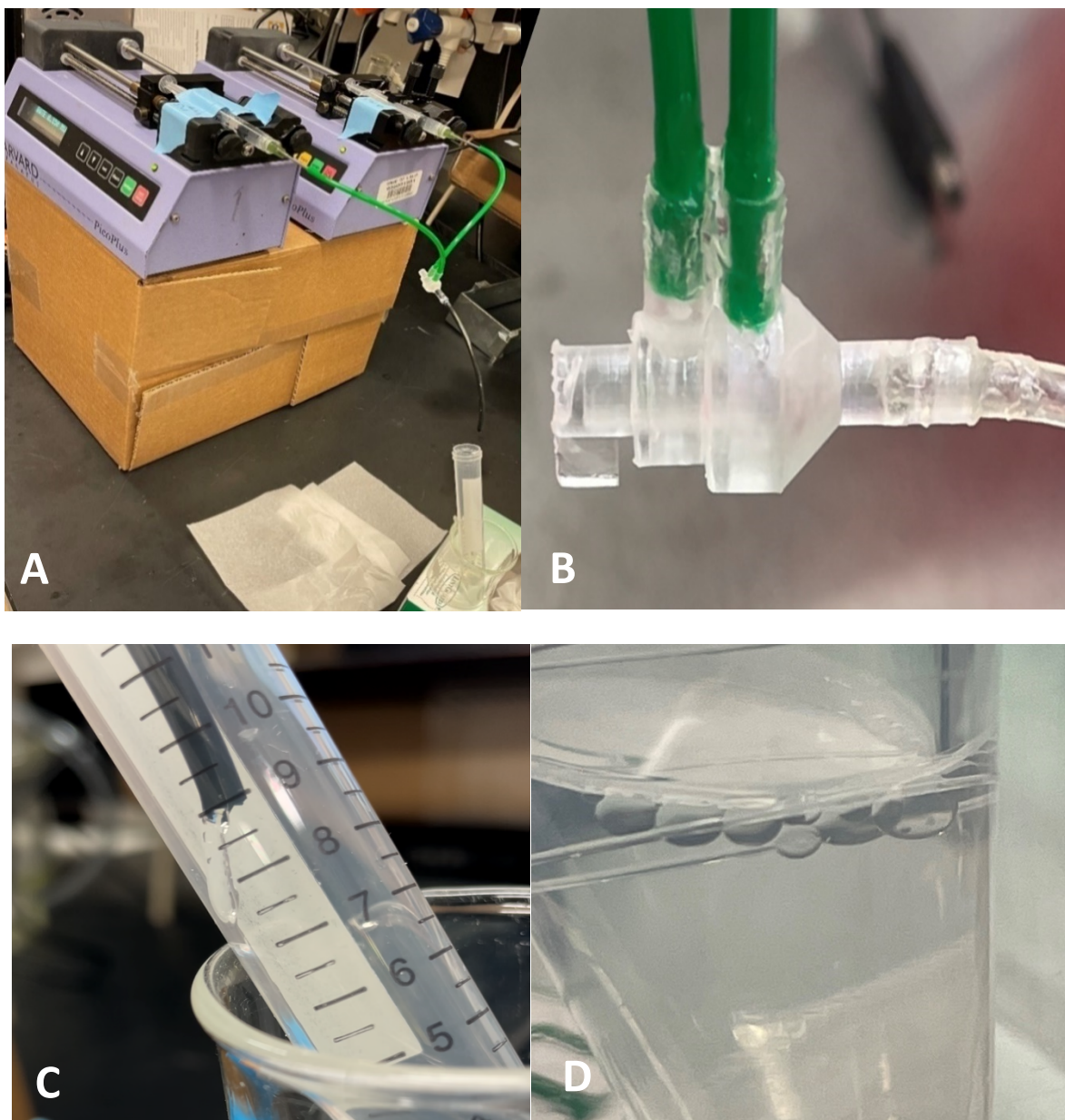
**Figure 4.2** Experimental setup used to test the droplet generator. (A) Syringe pumps were positioned on an elevated platform to minimize resistance to flow. A 15mL conical tube was used to collect the droplets and oil extruded from the outlet tubing. (B) Tubing was secured to the droplet generator head using super glue. Chamber A was also sealed with super glue to prevent backflow of Matrigel and oil. (C) A long strand of Matrigel is extruded into the 15mL collection tube. (D) Matrigel beads suspended just above the water phase.

Initial testing proved unsuccessful in producing Matrigel droplets. Instead, the Matrigel was extruded out in long strands that would occasionally be pinched off by the force of the oil. For the next round of testing, since the oil was already set to the maximum allowable flow rate of 0.15mL/min, the Matrigel flow rate would be dropped from 0.015mL/min to 0.01mL/min to promote bead formation through faster pinching of the Matrigel strand. Additionally, a 20mL syringe would be used for the oil-surfactant mixture to allow for a higher flow rate due to the increased cross-sectional area and diameter of the syringe. Despite 20mL syringes have diameters of 19.13mm, the syringe pumps were incorrectly calibrated to the 14.85mm diameter of a 10mL syringe, and it was later learned that the maximum programmable syringe diameter allowed by the pumps was 16mm. In the final optimized protocol, the use of a 20mL syringe set at a flow rate of 0.15mL/min for the oil mixture, and a 3mL syringe set at 0.01mL/min for the Matrigel mixture would yield the best conditions for the steady extrusion of similarly sized Matrigel beads.

For the second round of testing, cells were mixed with Matrigel. The same experimental setup shown in **Figure 4.2a** was used with slight alterations. A 50mL conical tube was used for the collection of droplets and oil, and media was filled into the conical tube in place of warm water. Droplets within a range of 100um to 900um diameters were obtained, however, initial imaging of the beads showed non-spherical bead formation. This was likely due to Matrigel not gelling properly in the warm media, despite the media having been warmed up to 37⁰C prior to experimentation. As a result of improper gelling, droplets were being deformed while pipetting them out of the conical collection tube. To mend this, after droplet extrusion, the collection tube containing the oil-mixture, media, and organoids was immediately sealed and placed in a 37⁰C incubator to allow for Matrigel gelation. After 5 minutes in the incubator, the collection tube was

opened, and the maximum allowable amount of oil-mixture and media were removed through pipetting. Some residual media and oil remained in-between the droplets. The remaining droplets were emptied onto a petri dish and imaged under a cell microscope. After a week, cancer organoids, also known as hollow cystic structures, were grown from the cells embedded in Matrigel. The presence of these 3D structures is an indicator that the cells were able to survive the encapsulation process and proliferate, since the initially encapsulated cell suspensions did not begin as large structures. The organoids were imaged and are shown in **Figure 4.4**.
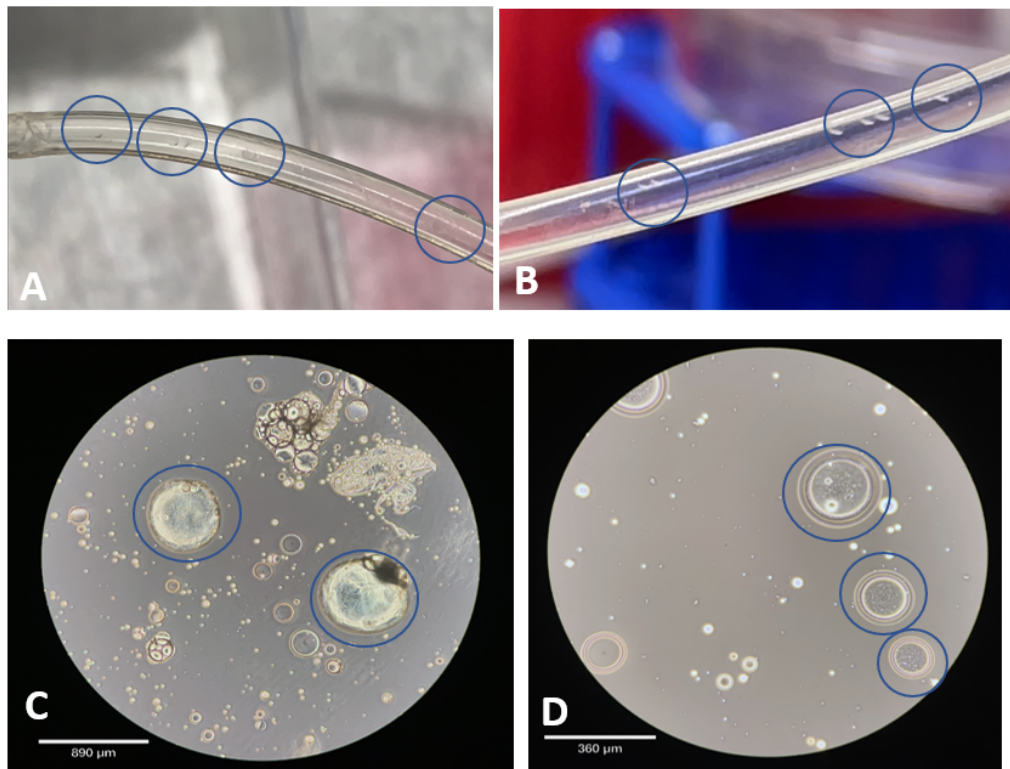


**Figure 4.3** Extrusion and microscope imaging of Matrigel droplets containing cancer cells. (A, B) Matrigel beads containing cells, circled in blue, are shown flowing through the clear outlet tube. (C, D) Matrigel beads under a microscope with some residual oil droplets in the background. Highlighted cell containing droplets are circled in blue. Cells are shown as white specs inside Matrigel beads. Microscope imaging was conducted in Dr. Halbrook's lab.
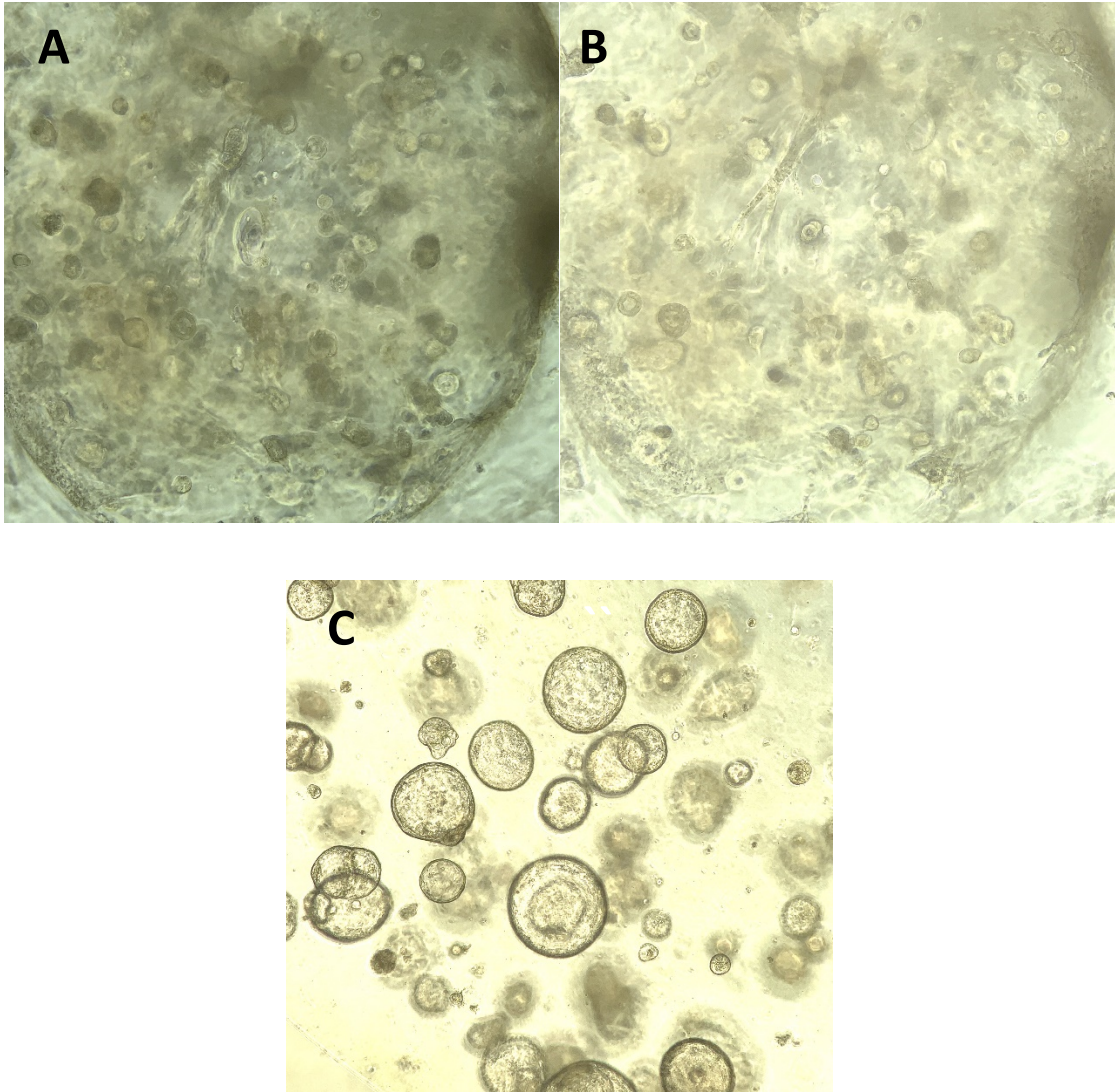
**Figure 4.4** Cancer organoids grown from cancerous cells in Matrigel beads. (A, B)

Cancer cells embedded in Matrigel beads grew into 3D – hollow cystic structures, referred to as

cancer organoids. Organoids grew from embedded cells in one week. Organoids were imaged in

Dr. Halbrook's lab. (C) Organoids grown in conventional Matrigel domes. Domes were placed

on flat culture plate to enable clear imaging.

Chapter 5: Conclusion

While SU-8 photoresist technology continues to be the primary means of fabrication used by microfluidics researchers, dry resist photolithography clearly has the potential to become just as widespread in use. The standardization of photoresist thickness coupled with the minimal instruments required for dry resist mold fabrication, and ease of access for researchers new to the field of microfluidics, are sure to make dry resist photolithography a growing trend in single and multi-layer device fabrication.

In this work, we demonstrated a novel multi-layer photolithography device fabrication technique using dry film photoresists. For standard SU-8 multi-layer fabrication, each photoresist layer is individually developed prior to the addition of new liquid SU-8 for the subsequent layer. The new SU-8 liquid flows over bumps and can fill cracks in the developed first layer. Since this procedure is not replicable with dry film laminate resists, and multi-layer device fabrication has never been attempted with dry film resists, we created a new method whereby the first layer of dry film resist was partially baked to reveal key patterns and alignment markers without the need for development of the first layer. We then demonstrated the use of a joint multi-layer alignment method whereby large alignment markers which were visible through semi-transparent photoresist layers, were used to roughly line up a first layer resist with a second layer photomask, and smaller markers were used to fine tune the alignment under a microscope. The use of this method repeatedly yielded an acceptable ≤50um alignment accuracy error for both the neuronal coculture device and the hydrophoretic filter device molds. We also demonstrated the optimization of key parts of the fabrication procedure such as UV exposure duration and PEB temperature ramp up and step duration. Thinner ADEX photoresists proved easier to work with

due to requiring shorter exposure and a simpler PEB procedure, while thicker SUEX resists were more sensitive to feature deformation, requiring a complex PEB.

After fabrication of the device master molds, PDMS devices were created through soft lithography and each device was tested. Testing of the neuronal coculture device showed successful migration of microglia from the annular chambers towards the inner chamber via thin microchannels. The hydrophoretic filter's branching outlet design was modeled unevenly and resulted in improper distribution of the outlet flow in a 1:2:2:1 ratio. For our tests, an edge-cut outlet design was utilized, allowing polystyrene microcarriers and murine pancreatic cancer cells to flow out of the device outlet evenly without hindering hydrophoresis. Edge-cut device testing showed successful lateral distribution of 125-212um diameter beads towards the lower half of the outlet chamber. When testing the device with cancer cells, a slight upper stream of concentrated cells formed in the outlet chamber, showing that some cells were being sorted to their proper lateral position. However, a majority cell tests showed inconsistent results due to cells flowing evenly throughout the entire span of the outlet chamber. In future work, the branching outlet design needs to be reconfigured, and cell tests need to be repeated to see if hydrophoresis with particles ≤100um in diameter is possible for the device.

Finally, a droplet generator device was successfully used to develop Matrigel droplets containing cancer cells with slight droplet diameter variability. Cancer organoids were later grown from the Matrigel droplets. To further optimize the droplet generation process in the future, new syringe pumps should be used which allow for a higher programmable syringe diameter size. This would allow the proper use of a 20mL syringe for the oil-surfactant mixture to be pumped at a correct speed. New syringe pumps with a maximum allowable flow rate of 1mL/min would allow the droplet generator to be run with the original intended flow rates for oil

and Matrigel, possibly resulting in higher frequency generation of droplets with less diameter

variability.

REFERENCE

[1] Park, Joseph, et al. "A 3D human triculture system modeling neurodegeneration and neuroinflammation in Alzheimer's disease." Nature neuroscience 21.7 (2018): 941-951.

[2] Cho, Hansang, et al. "Microfluidic chemotaxis platform for differentiating the roles of soluble and bound amyloid-β on microglial accumulation." Scientific reports 3.1 (2013): 1-7.

[3] Cho, Hansang. "Mimicry of neuroinflammatory microenvironments and methods of use and manufacturing thereof." U.S. Patent Application No. 15/670,354.

[4] Choi, Sungyoung, et al. "Sheathless focusing of microbeads and blood cells based on hydrophoresis." Small 4.5 (2008): 634-641.

[5] Choi, Sungyoung, et al. "Hydrophoretic high-throughput selection of platelets in physiological shear-stress range." Lab on a Chip 11.3 (2011): 413-418.

[6] Mata, Alvaro, Aaron J. Fleischman, and Shuvo Roy. "Fabrication of multi-layer SU-8 microstructures." Journal of micromechanics and microengineering 16.2 (2006): 276.

[7] Mukherjee, Prithviraj, et al. "Rapid prototyping of soft lithography masters for microfluidic devices using dry film photoresist in a non-cleanroom setting." Micromachines 10.3 (2019): 192.

[8] Roos, Michael M., et al. "Towards Green 3D-Microfabrication of Bio-MEMS Devices Using ADEX Dry Film Photoresists." International Journal of Precision Engineering and Manufacturing-Green Technology (2021): 1-15.

[9] Puzzo, Daniela, et al. "Picomolar amyloid-β positively modulates synaptic plasticity and memory in hippocampus." Journal of Neuroscience 28.53 (2008): 14537-14545.

[10] Choi, Sungyoung, et al. "Microfluidic self-sorting of mammalian cells to achieve cell cycle synchrony by hydrophoresis." Analytical chemistry 81.5 (2009): 1964-1968.

[11] Kleinman, Hynda K., and George R. Martin. "Matrigel: basement membrane matrix with biological activity." Seminars in cancer biology. Vol. 15. No. 5. Academic Press, 2005.

[12] Drost, Jarno, and Hans Clevers. "Organoids in cancer research." Nature Reviews Cancer 18.7 (2018): 407-418.

[13] Sachs, Norman, et al. "A living biobank of breast cancer organoids captures disease heterogeneity." Cell 172.1-2 (2018): 373-386.

[14] Hopperton, K. E., et al. "Markers of microglia in post-mortem brain samples from patients with Alzheimer's disease: a systematic review." Molecular psychiatry 23.2 (2018): 177-198.

[15] Heneka, Michael T., et al. "Neuroinflammation in Alzheimer's disease." The Lancet Neurology 14.4 (2015): 388-405.

[16] ADEXR Epoxy Thin Film Rolls/Sheets - DJ Microlaminates.

https://djmicrolaminates.com/wp-content/uploads/2020/08/DJML-ADEX-Data-Sheet.pdf.

[17] Choi, Sungyoung, et al. "Continuous blood cell separation by hydrophoretic filtration." Lab on a Chip 7.11 (2007): 1532-1538.

[18] Choi, Sungyoung, and Je-Kyun Park. "Continuous hydrophoretic separation and sizing of microparticles using slanted obstacles in a microchannel." Lab on a Chip 7.7 (2007): 890-897.

[19] Choi, Sungyoung, et al. "Hydrophoretic sorting of micrometer and submicrometer particles using anisotropic microfluidic obstacles." Analytical chemistry 81.1 (2009): 50-55.

[20] Johnson, Donald W. et al. "SUEX for high aspect ratio micro-nanofluidic applications." (2012).

[21] Hughes, Chris S., Lynne M. Postovit, and Gilles A. Lajoie. "Matrigel: a complex protein mixture required for optimal growth of cell culture." Proteomics 10.9 (2010): 1886-1890.

[22] Ghaznavi, Amirreza, et al. "A Monolithic 3D Printed Axisymmetric Co-Flow Single and Compound Emulsion Generator." *Micromachines* 13.2 (2022): 188.